

ALOS, ALOS-2 and Solid Earth Observations

Masanobu Shimada, Dr.

Japan Aerospace Exploration Agency
Earth Observation Research Center

Dec. 22, 2011

PIXEL workshop at Kyoto University

Contents of my talk

- ALOS and mission objectives
- CALVAL and features
- Data Acquisitions
- InSAR and Performance Evaluation
- Coherence vs. incidence angle
- Ionospheric perturbation
- ScanSAR InSAR
- ALOS-2
- Conclusion

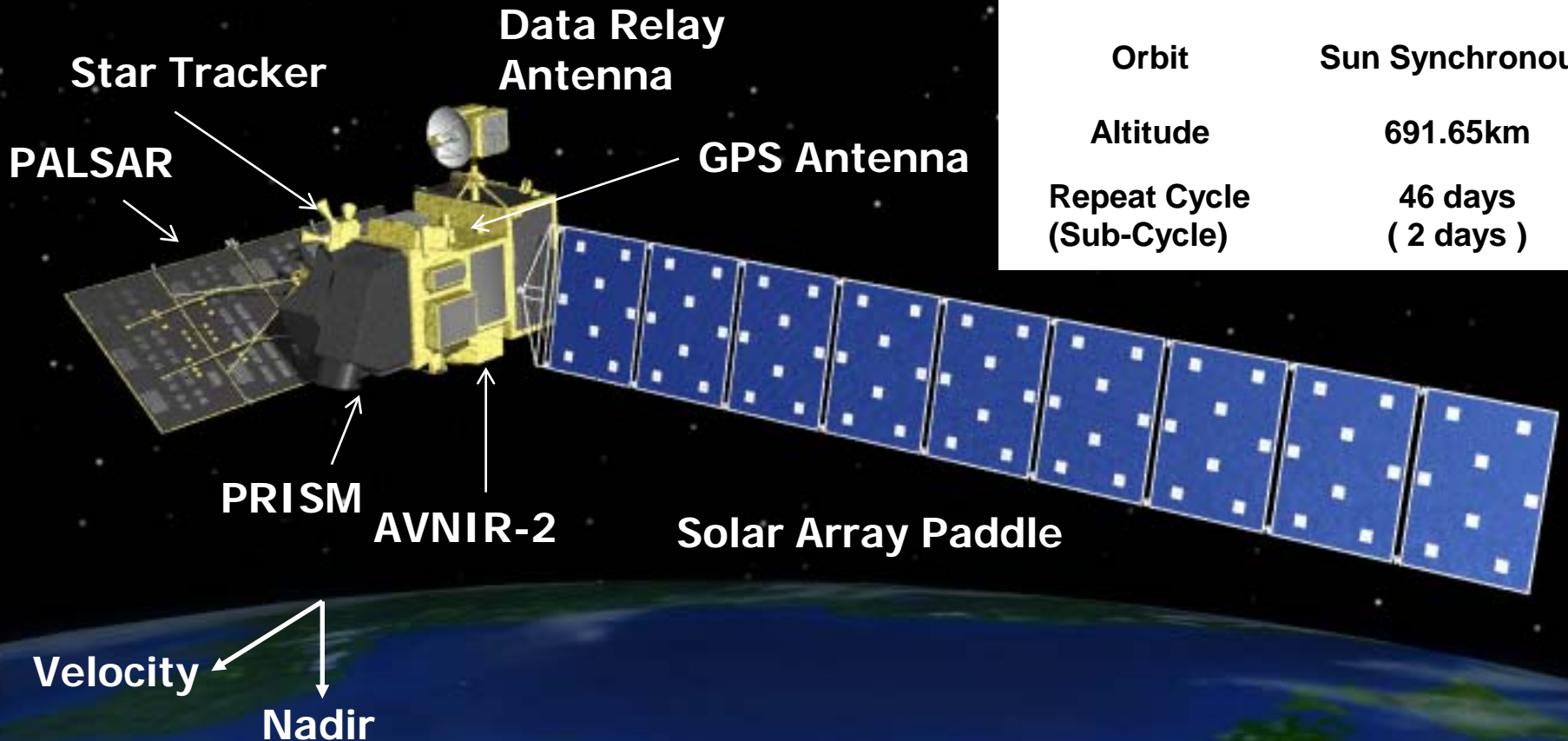
ALOS Satellite System

Launch Date	Jan. 24 2006
Launch Vehicle	H-IIA
Spacecraft Mass	about 4,000kg
Generated Elec. Power	about 7kW at EOL

Orbit Sun Synchronous

Altitude 691.65km

Repeat Cycle (Sub-Cycle) 46 days (2 days)



PRISM : Panchromatic Remote-sensing Instrument for Stereo Mapping

AVNIR-2: Advanced Visible and Near Infrared Radiometer type 2

PALSAR: Phased Array type L-band Synthetic Aperture Radar

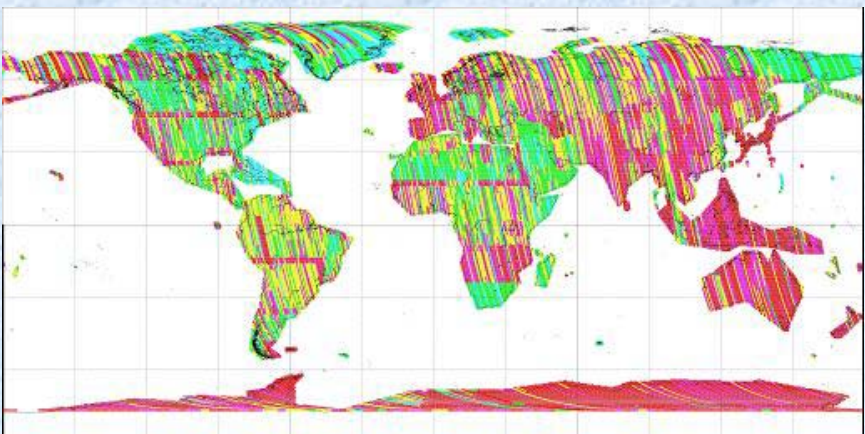
センサーと衛星の特性

- PALSAR (L-band SAR, 14/28MHz, STRIP(FBS, FBD, Pol), ScanSAR)
- AVNIR-2(4 band 光学)
- PRISM(Pan-DSM 光学)
- 正確な位置精度とラジオメトリ
- 高い安定性
- 長時間の観測 (~50 min./1軌道)
- 静止データ中継衛星を用いた全球観測
DRTS + TDRS(650万シーン/ 1 PB / 5 年)
- 基本観測シナリオ

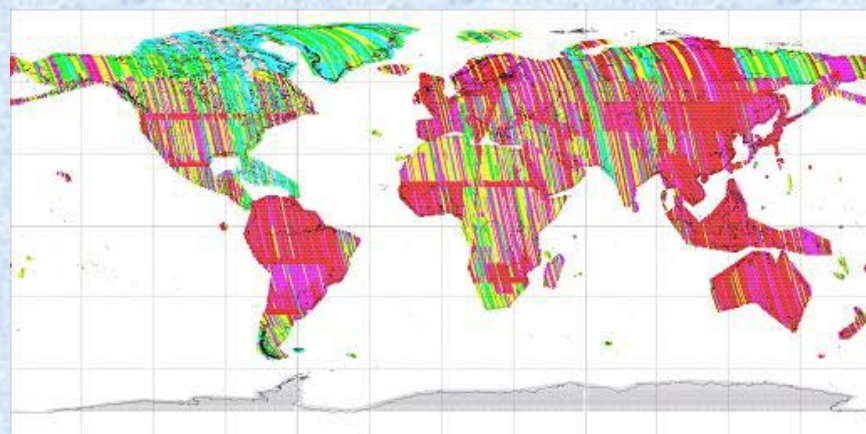
Applications (応用事例)

- Oil Spill (海上油汚染)
- Fire scare (森林火災)
- Flooding (洪水)
- Land Slide (Flash water and Slow moving) (地滑り)
- Subsidence (地盤沈下)
- Volcano (火山)
- Earthquake (地震)
- Forest, REDD+, Wetland (森林監視)
- Polar Ice/Glaciers (極域氷河)
- Coastal Erosions (海岸浸食)
- Drift Ice monitoring (流氷)
- Change Detections (変化抽出)
- Rice Paddy Monitoring (作付け面積)
- Illegal Logging Monitoring (違法森林伐採監視)
- Ocean Wind Speed distribution (海上風速分布)
- DSM generation (PRISM, PALSAR by InSAR) (標高データ作成)
- Ionospheric Disturbances (電離層分布)
- Radio Frequency Interference (周波数干渉)
- Ortho-rectification (オルソ画像)
- Soil Moisture (土壤水分)

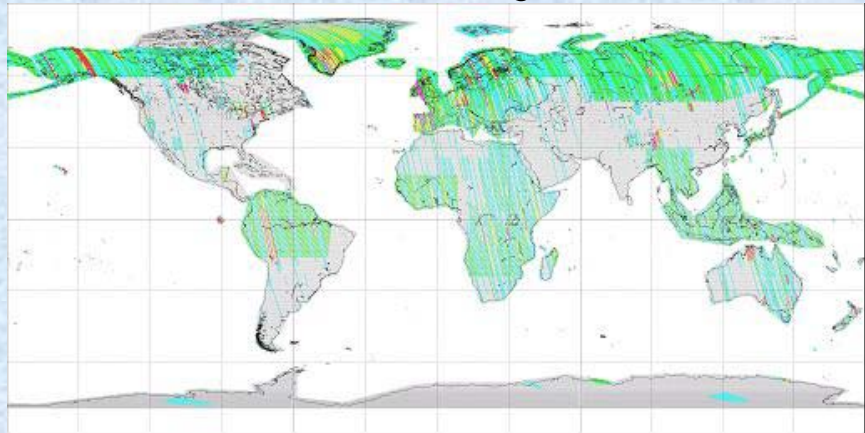
Global Data Acquisition and Basic Observation Scenario



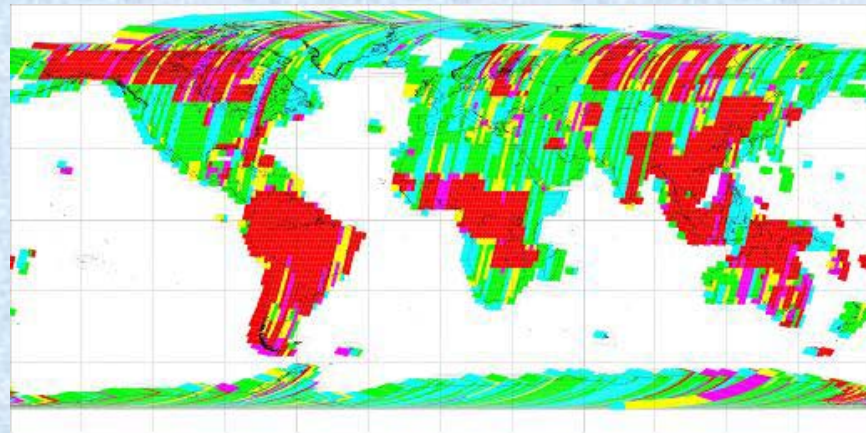
FBS Off-nadir:34.3deg (ascend)



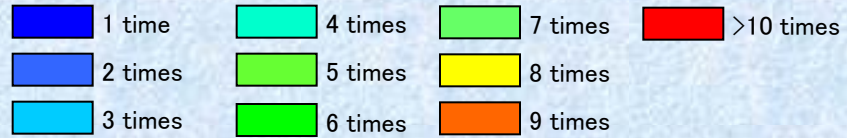
FBD Off-nadir:34.3deg (ascend)



PLR Off-nadir:21.5deg (ascend)



WB1/WB2 Off-nadir:27.1deg (descend)



Duration: 2006年5月16日 ~ 2011年1月23日

PALSAR Data archives as of Jan. 23 2011

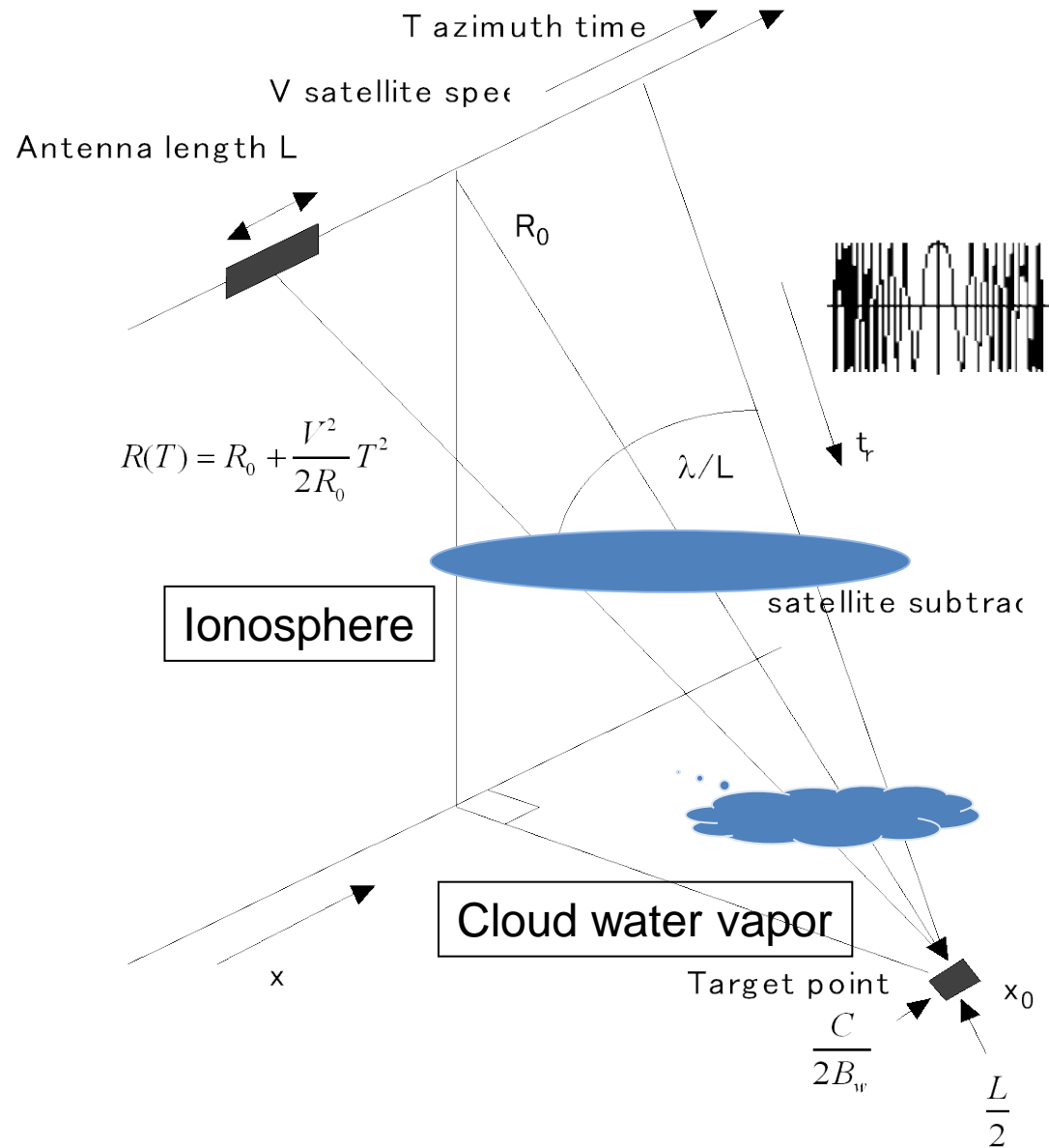
L-band SAR Characteristics

- Advantages (than higher frequency)
 - Higher Penetration through the vegetation covered targets
 - High InSAR coherence for the vegetation covered target
 - Lower backscatter from the lower vegetation
- Disadvantage (and advantage)
 - Higher sensitivity to the ionospheric disturbance

SAR imaging

High resolution SAR imaging is performed by two scale correlation processes, i.e., FM modulation in range and Doppler modulation in azimuth.

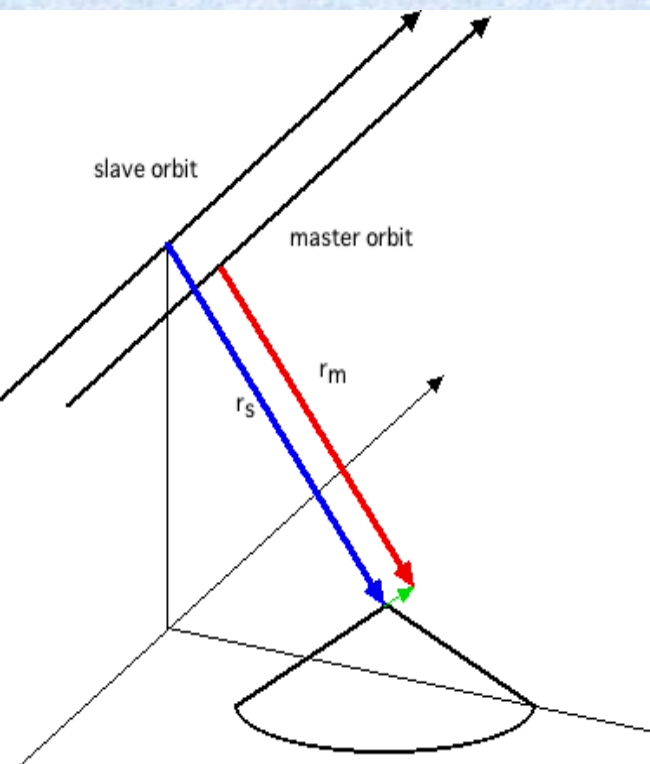
	Bw	L
JERS-1	15M	12m
PALSAR	28M	9m
PALSAR	14M	9m
Pi-SAR-L	50M	1.6m



$$S_{ra}(R, x) = A(R, x) \operatorname{sinc} \left(\frac{2\pi B_w (R - R_0)}{c} \right) \operatorname{sinc} \left(2\pi \left(\frac{x - x_0}{L} \right) \right) \exp \left(-\frac{4\pi R_0}{\lambda} j \right)$$

Differential SAR interferometry (1/2)

obtain the surface deformation map by differentiating two SAR images acquired at different times(master and slave), by correcting the distances between two orbits (1), and by correcting the surface topography (2).



coordinate system

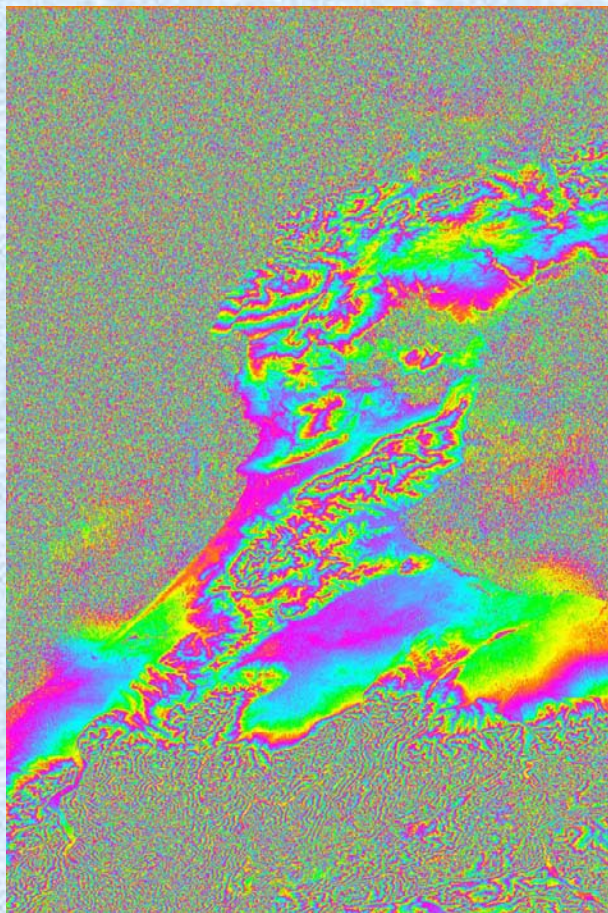


master(4/10/2007)

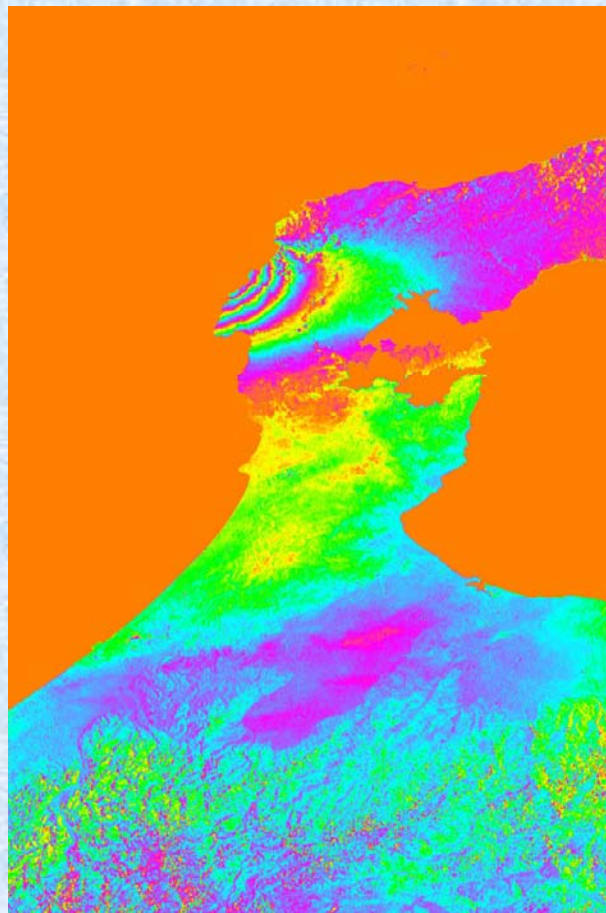


slave(2/23/2007)

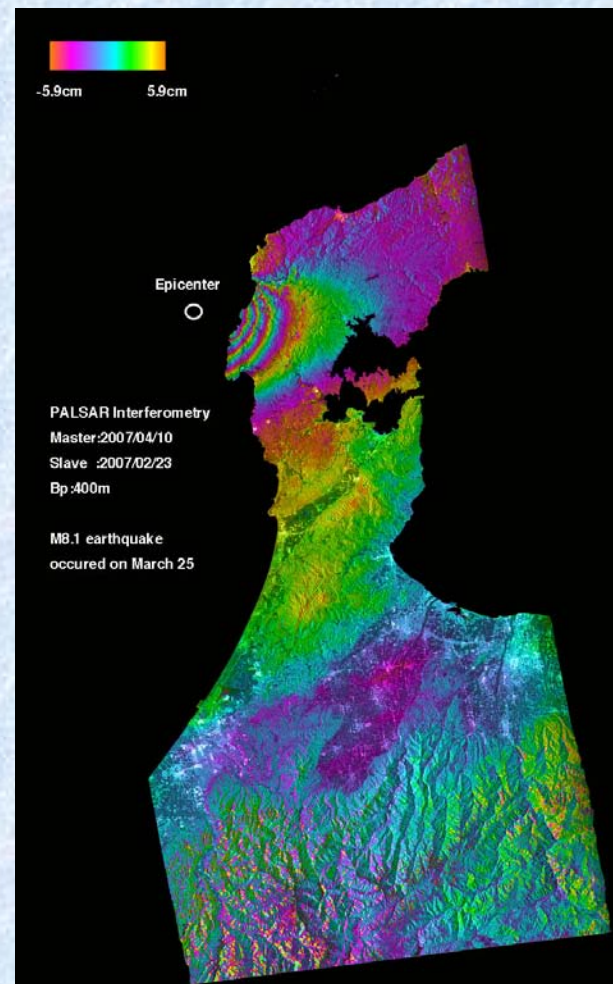
Final result (3) is gained by ortho-rectification and the geocoding of the image (2)



(1) orbit correction



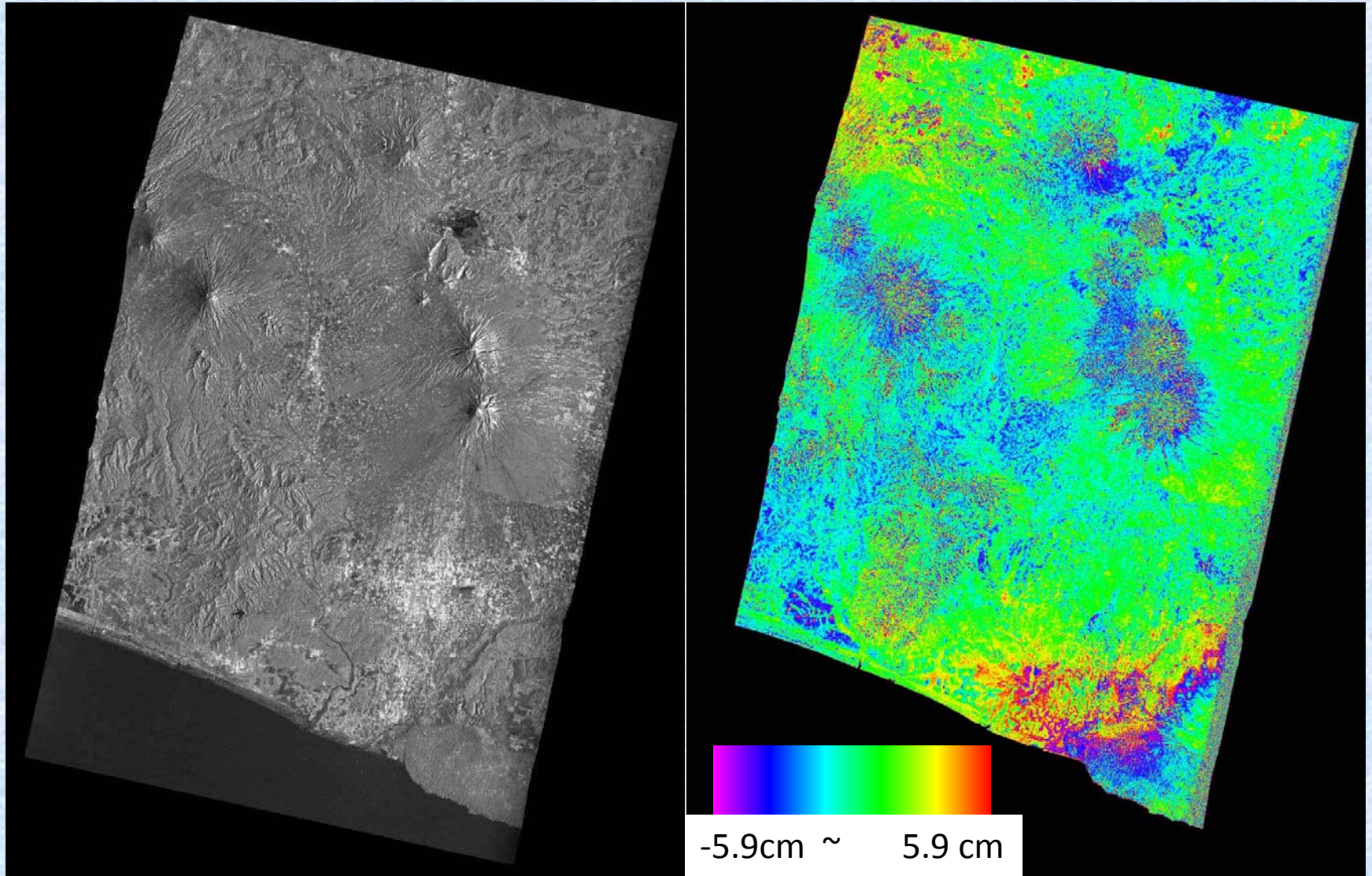
(2) topography correction



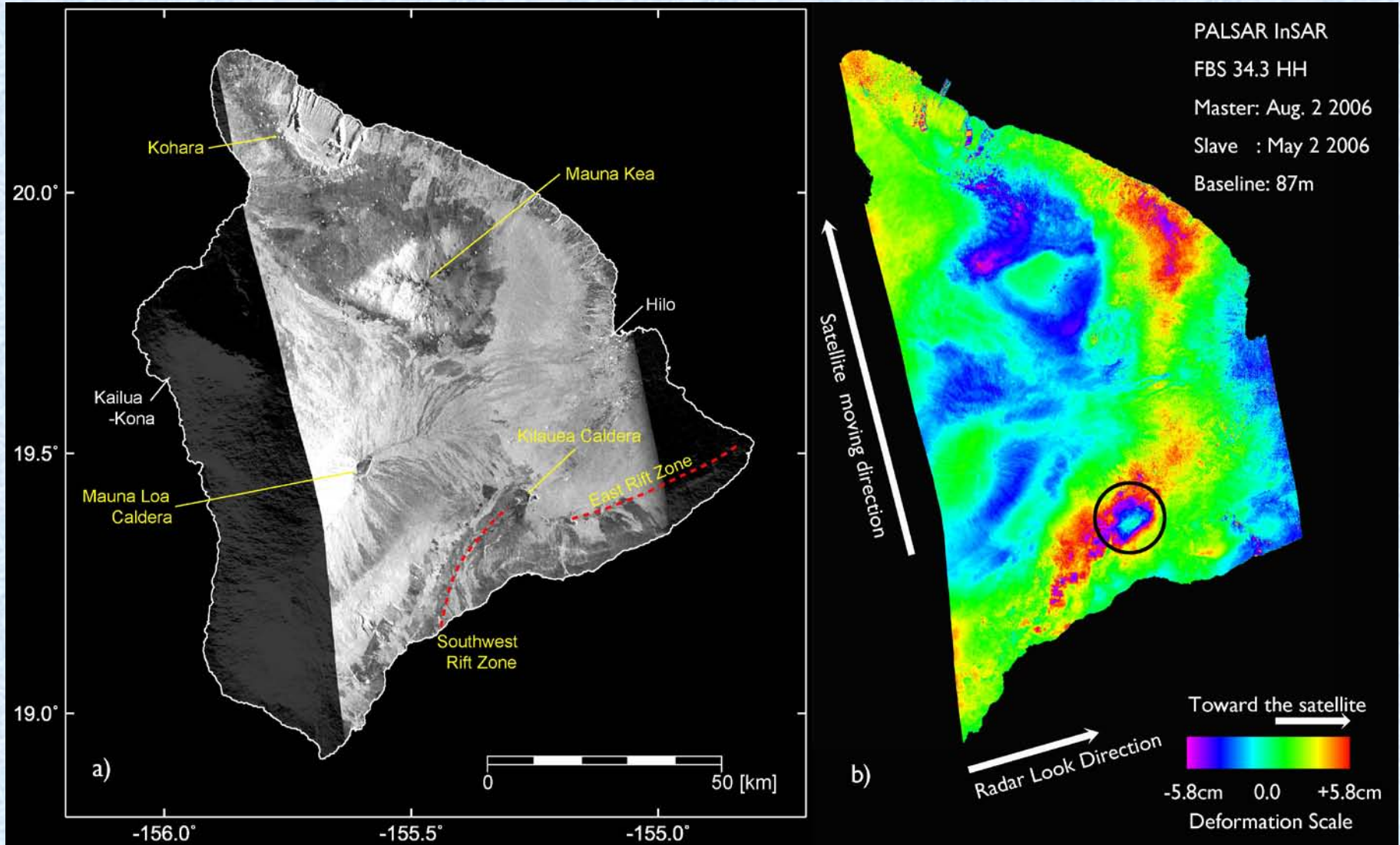
(3) final result

Yogyakarta- First detection

Indonesia, Earthquake triggered by Mt. Merapi Volcano, April 2006



First DinSAR image detected by the PALSAR over Hawaii



Noto Earthquake

Case 1

2007年04月10日

2007年02月23日

Yaw steer OFF

off=41.5

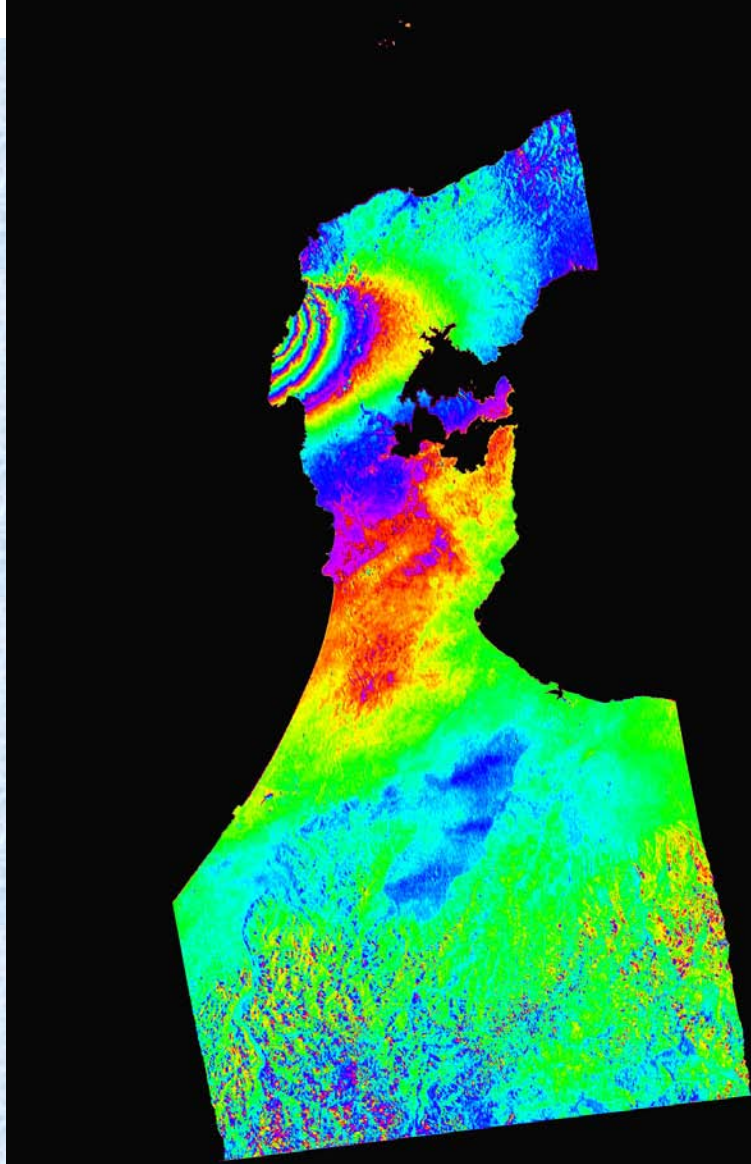
Case 2

2007年05月10日

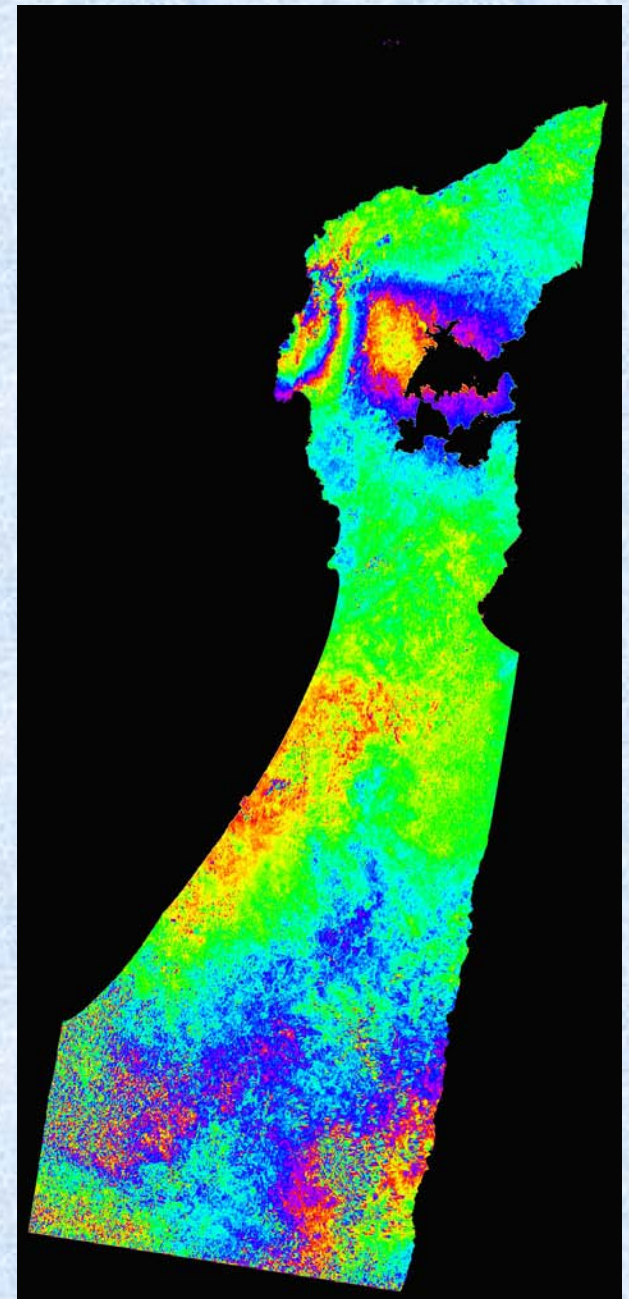
2006年12月23日

Yaw steer ON

off=34.4

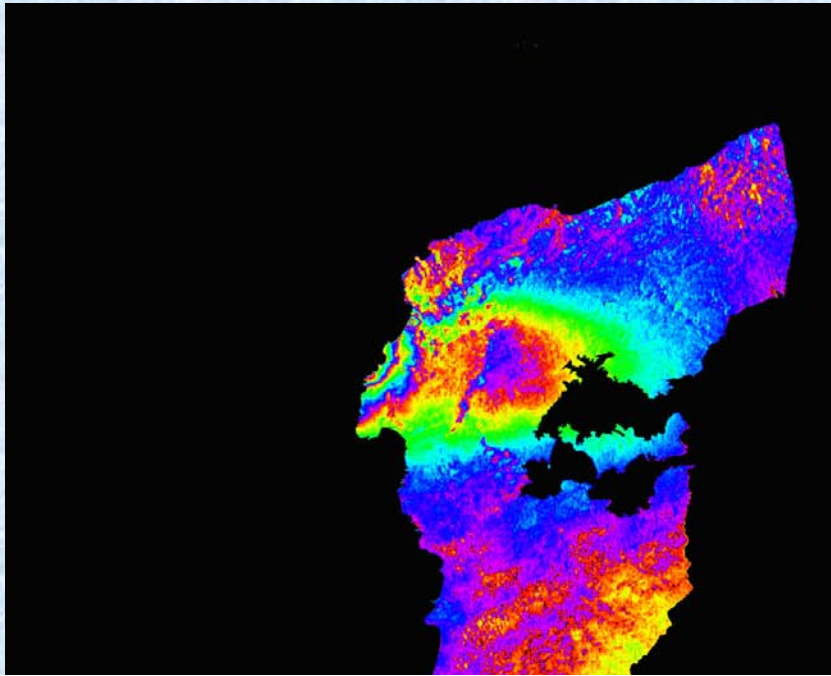


C1. Ascending Orbit

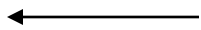
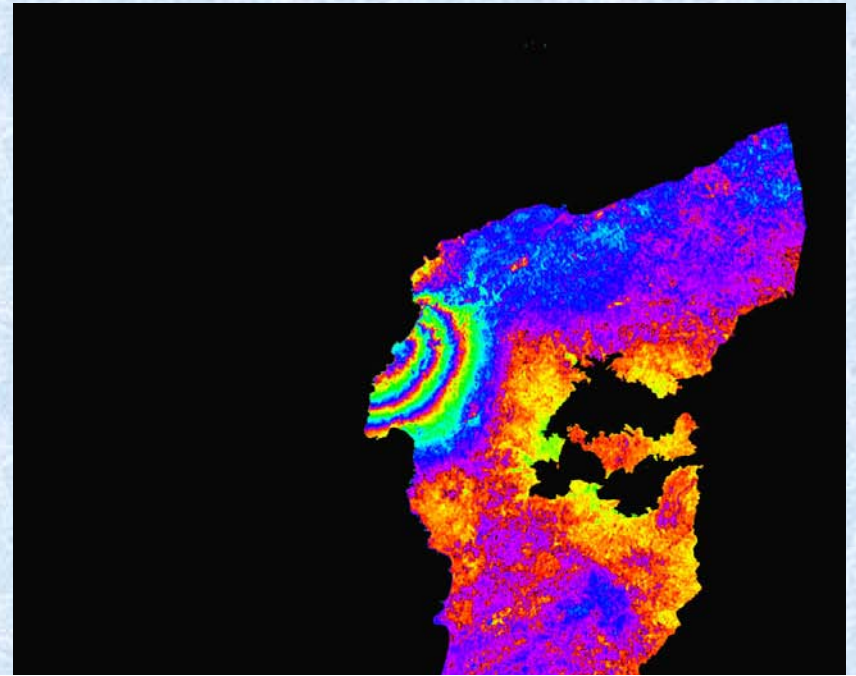


C2. Descending Orbit

水平方向変位

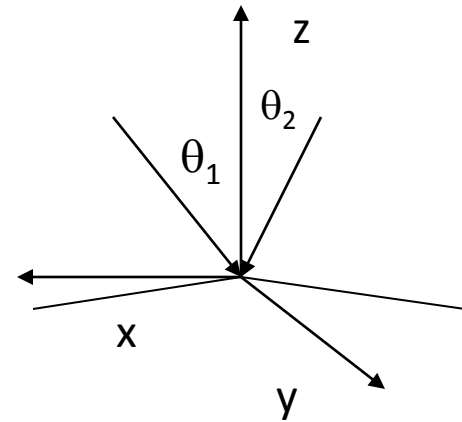


垂直方向変位



$$x = (d_1 - z \cos \theta_1) / (\cos \phi \cos \theta_1)$$
$$z = (d_1 \sin \theta_2 + d_2 \sin \theta_1) / \sin(\theta_1 + \theta_2)$$

変化はxとzのみと仮定



Solomon Island

M8.1

April 2 2007

Three DinSAR

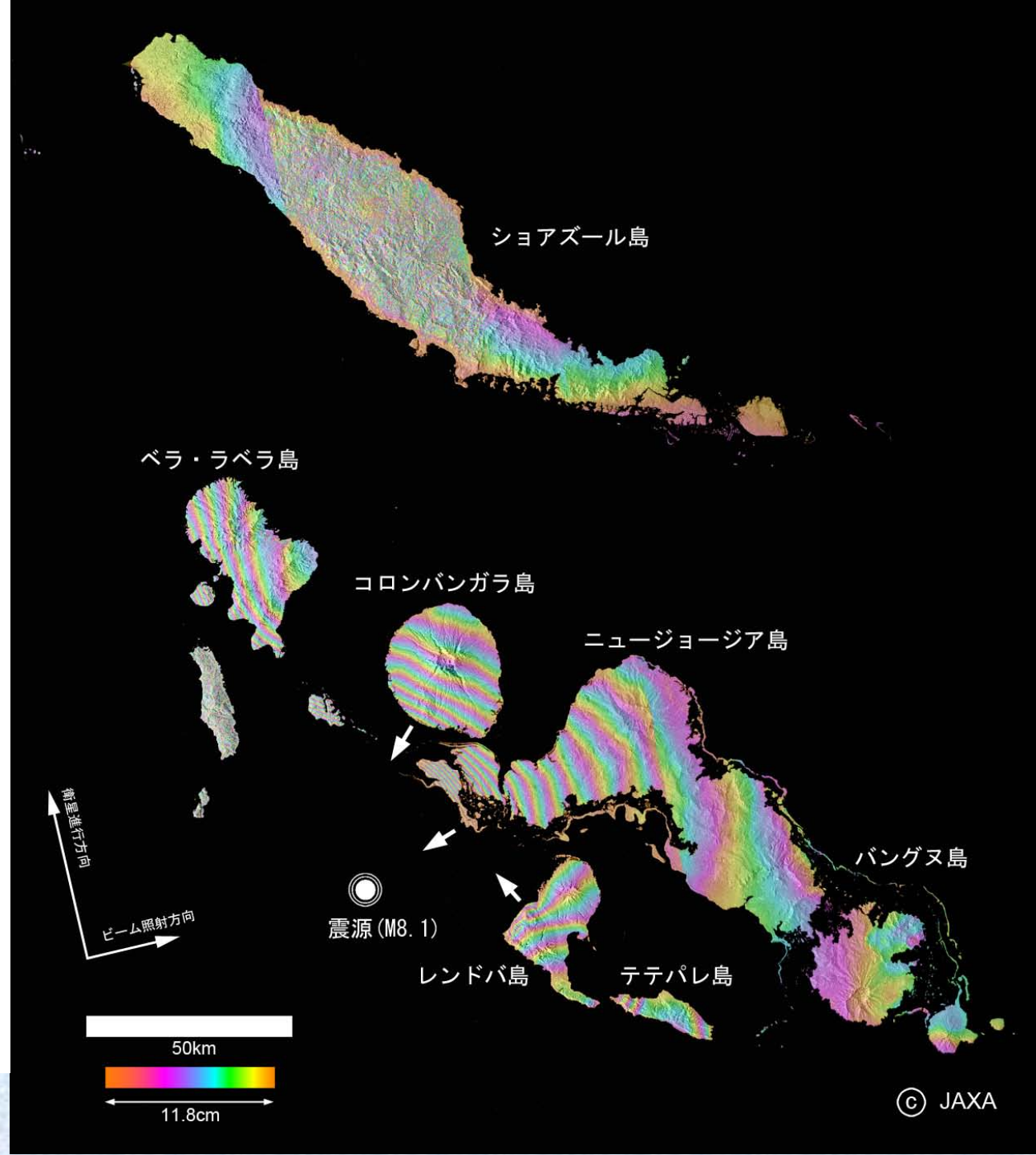
344:4/10-2/23

345:5/3-1/31

343:5/10-2/12

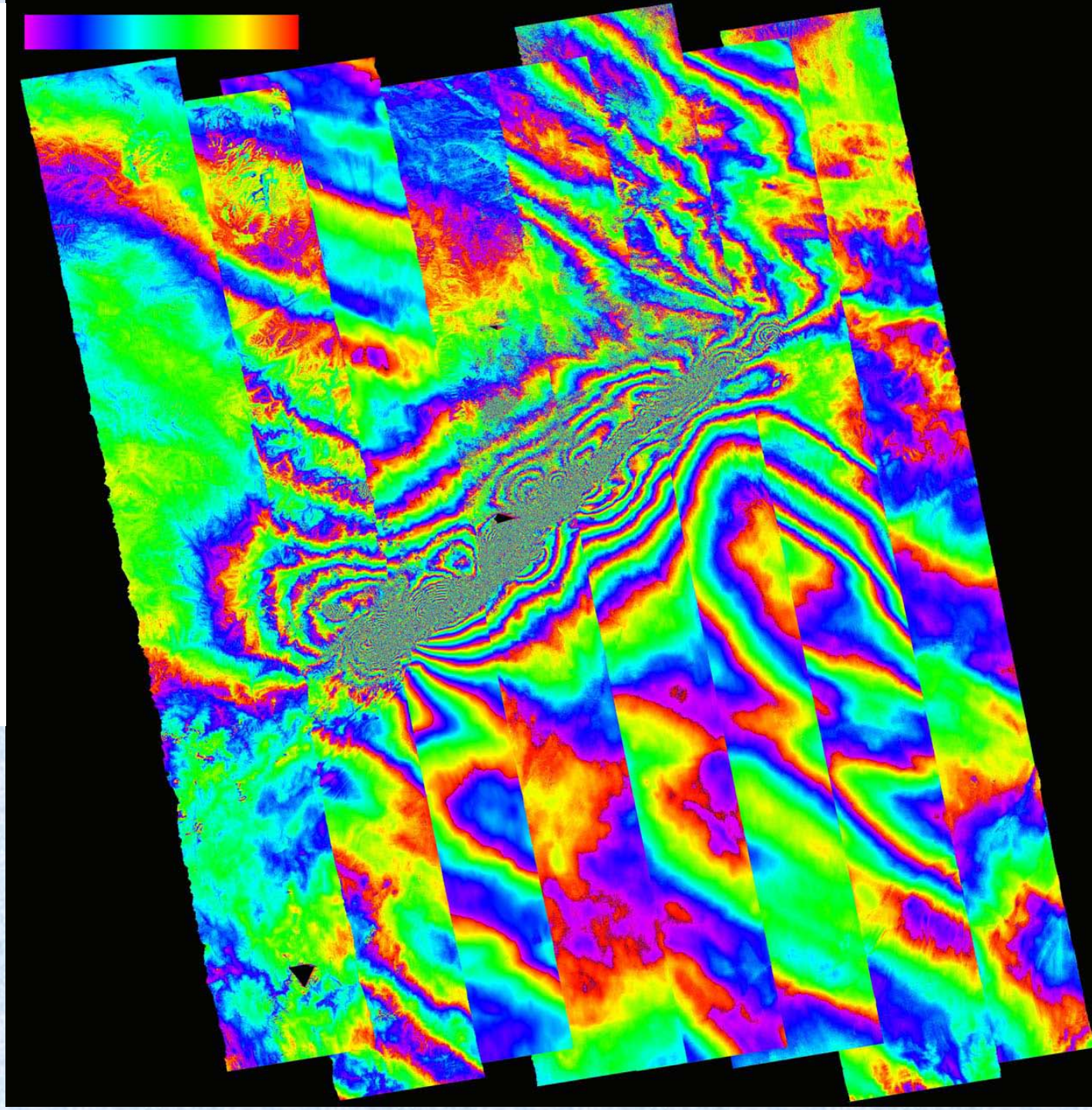
FBS343HH

- No orbit tuning.
- No further correction
- Three passes mosaic



May 12 2008
Wunshen
Earthquake
PALSAR data
8 pass mosaic

- First detection of the 290km faults
- All ascending passes
- Noisy patterns due to the ionosphere

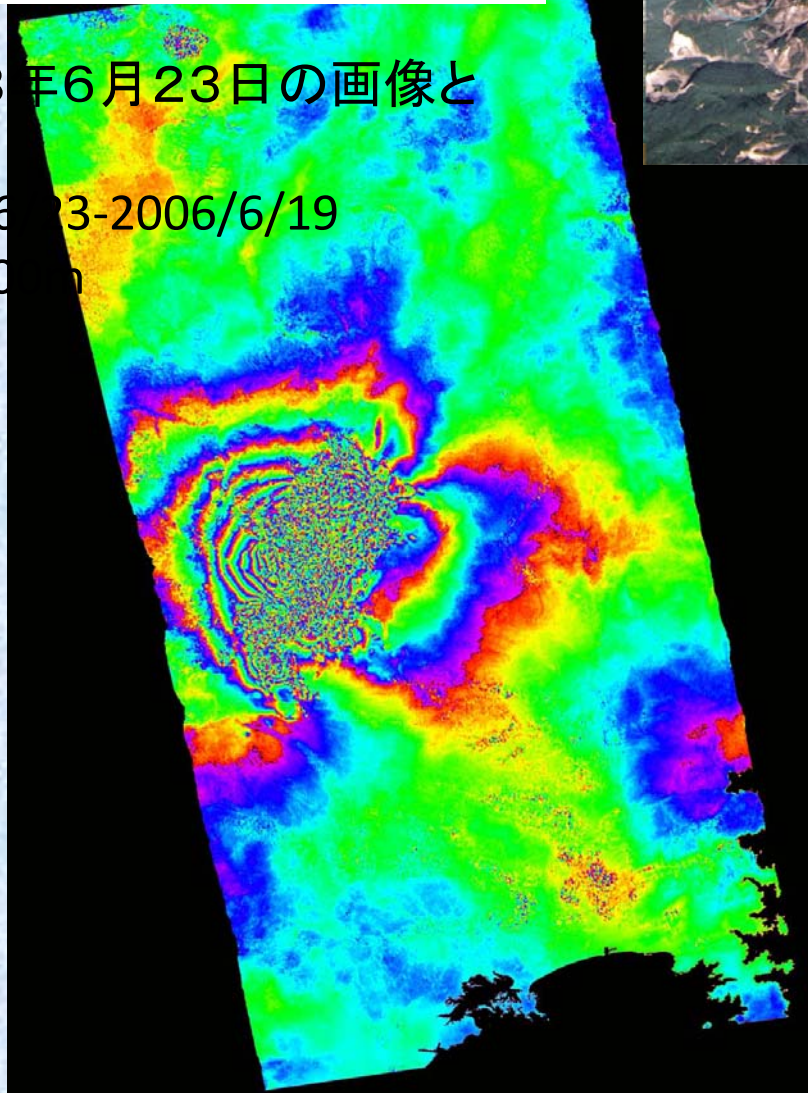


Iwate Miyagi Earthquake

2008年6月23日の画像と

2008/6/23-2006/6/19

Bp=-50



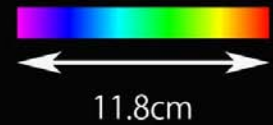
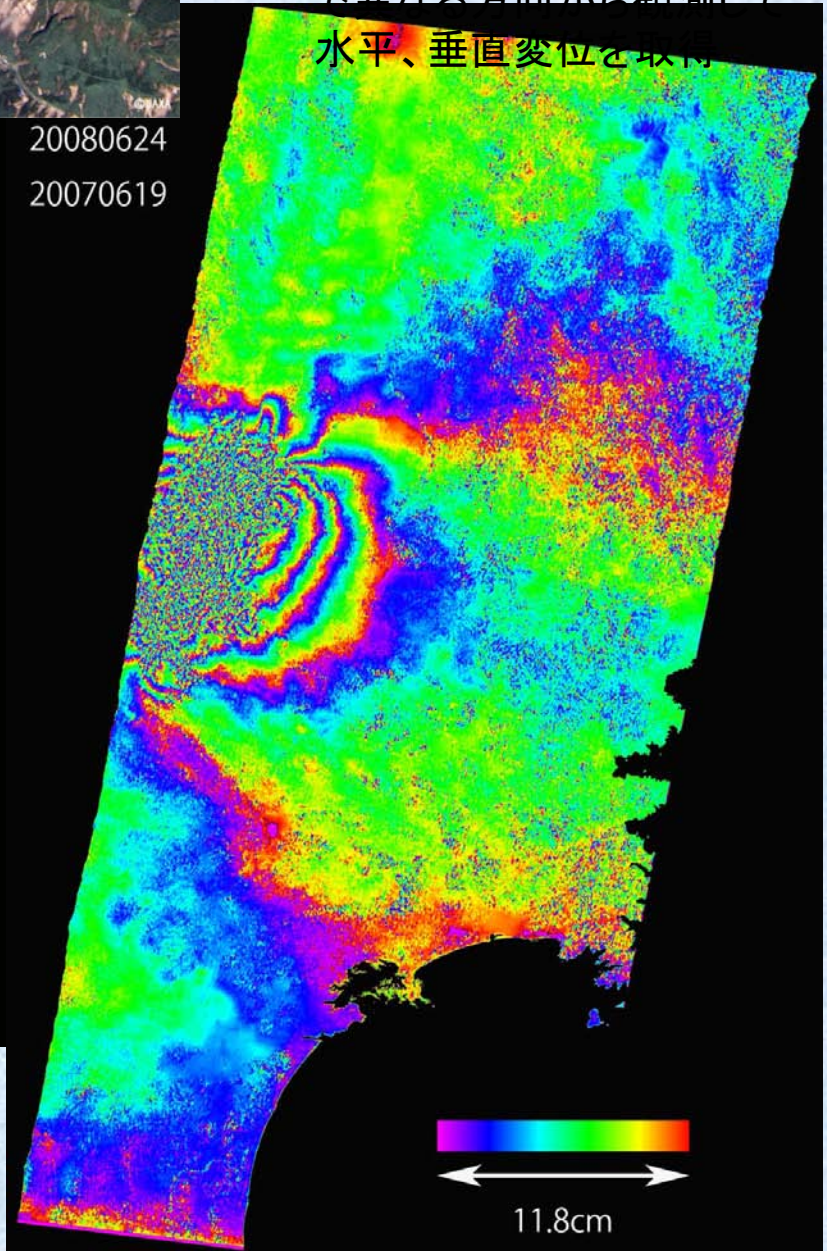
20080624

20070619

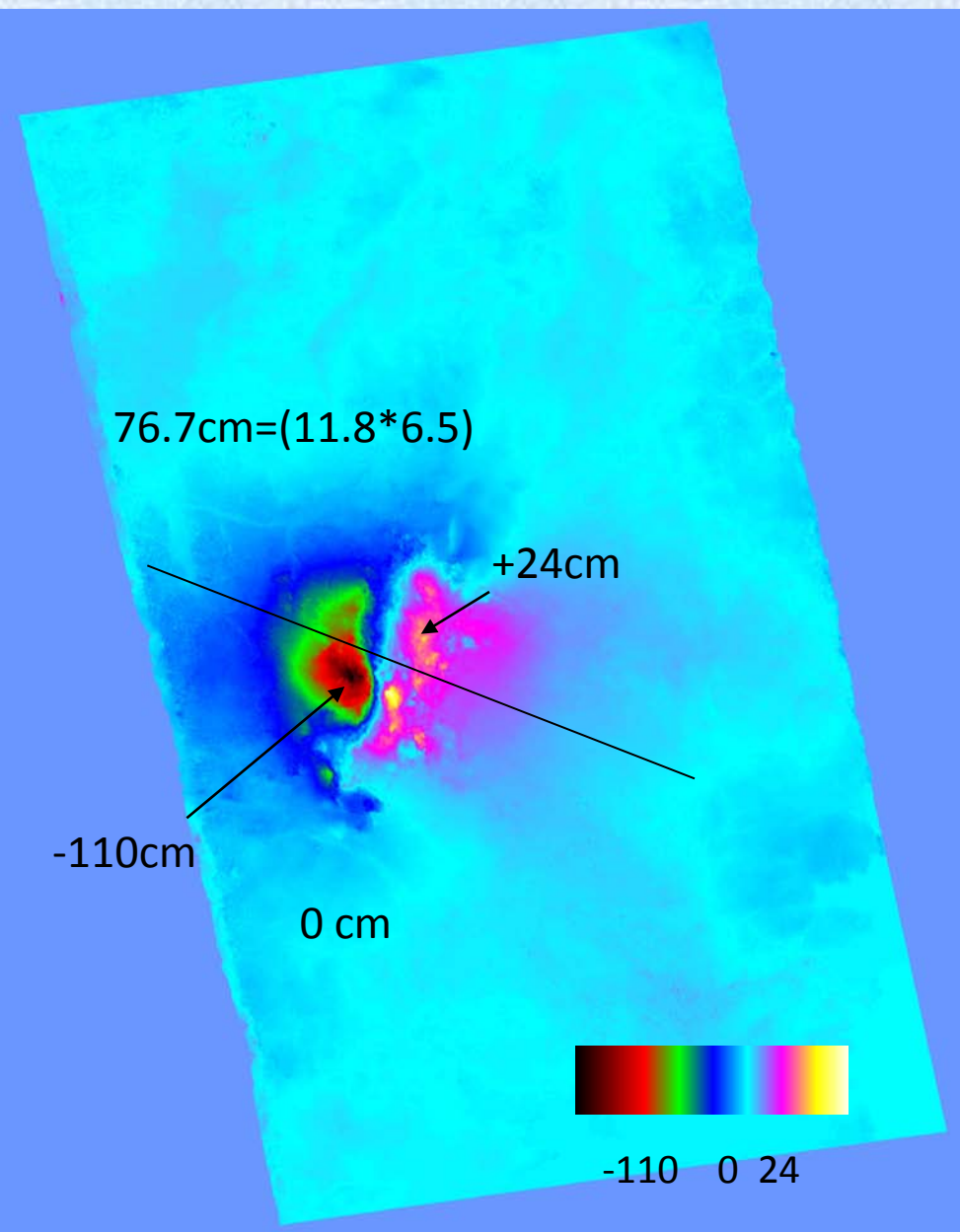
2008/6/24

2007/6/19

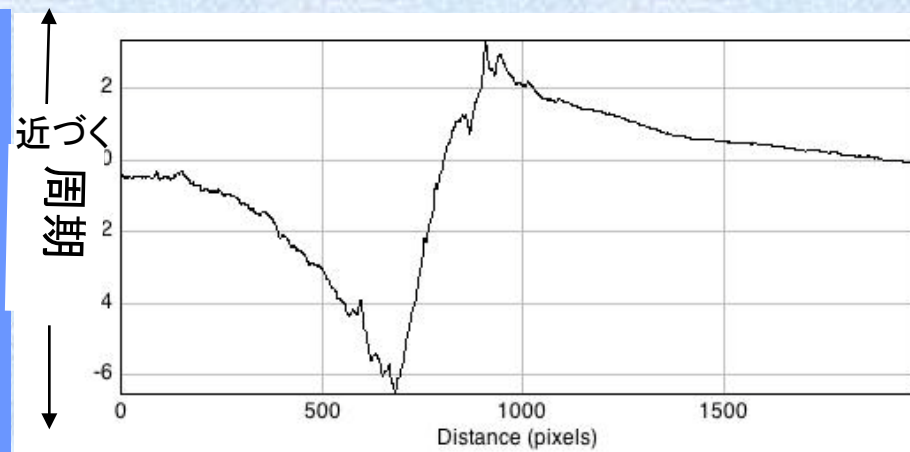
異なる方向から観測して
水平、垂直変位を取得



(Unwrapped data)

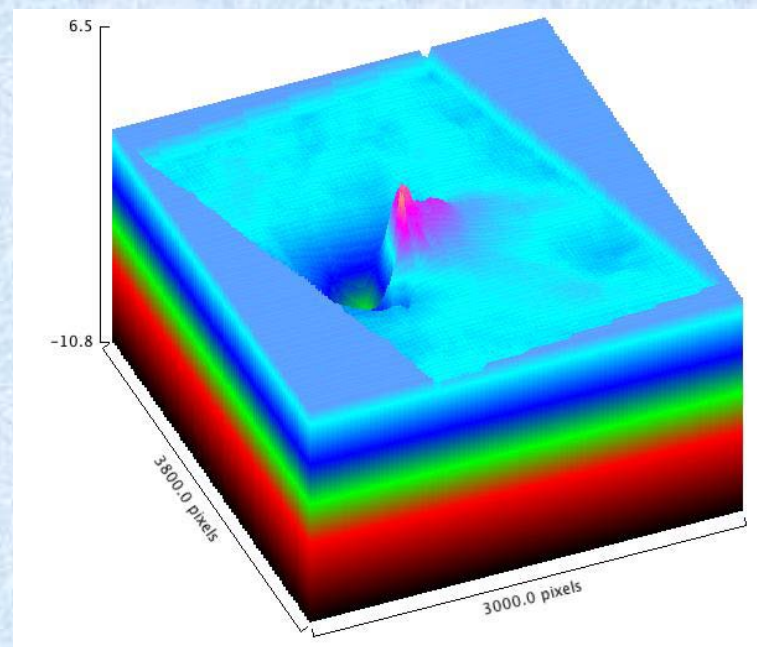


Unwrapped phase



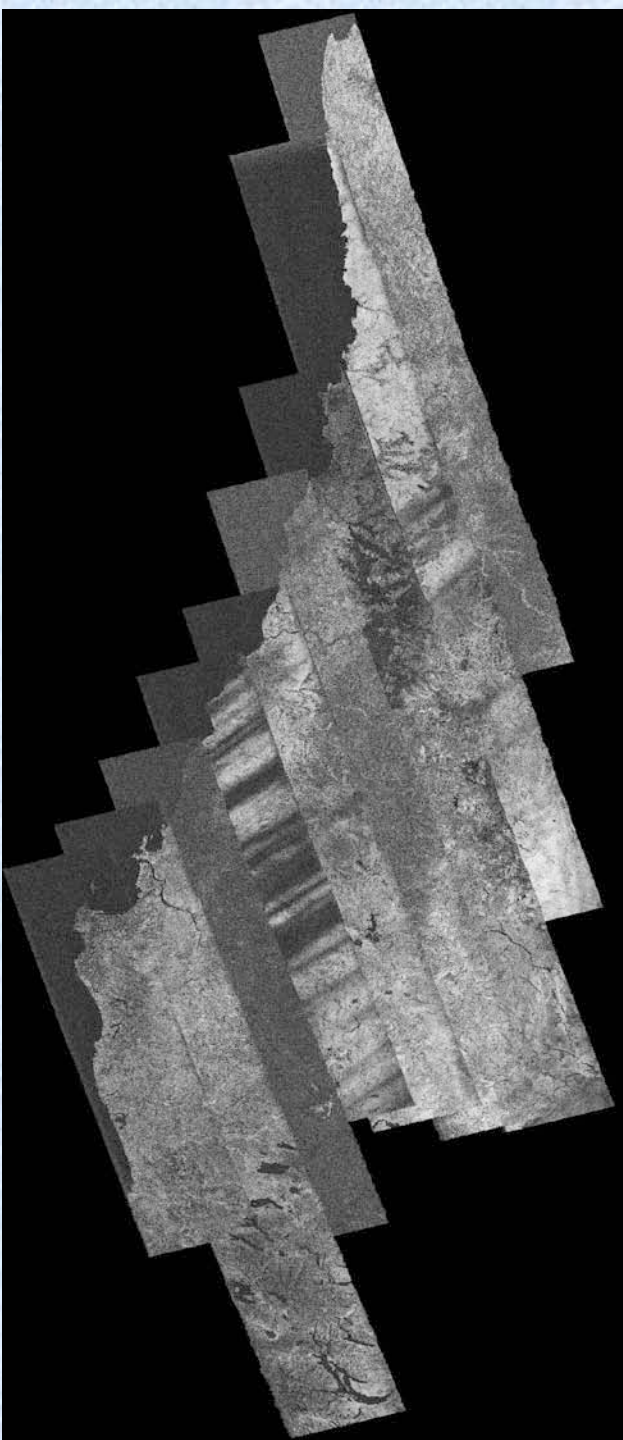
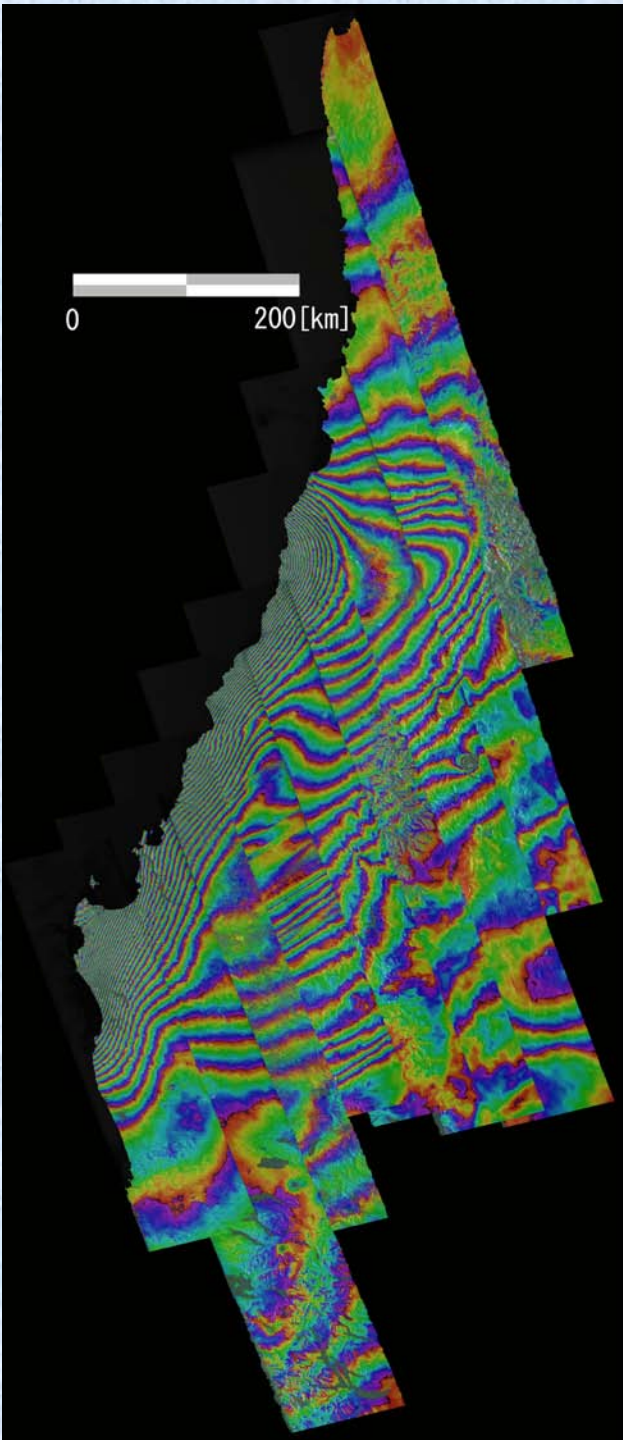
変動量の断面図/Cross section

遠ざかる



変化量を積分したもの(3次元図)

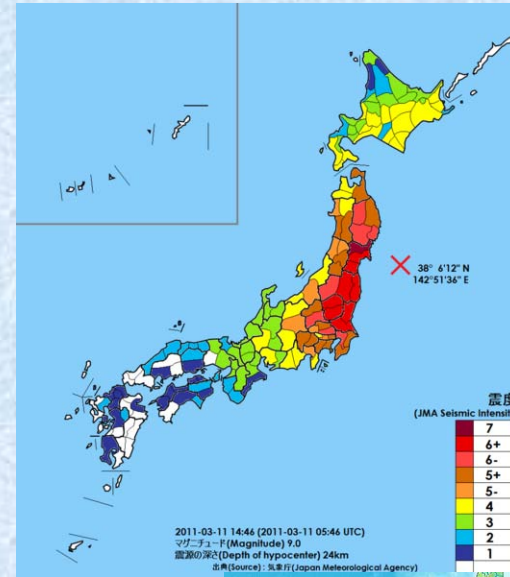
Deformation monitoring for Chile Earthquake 2010



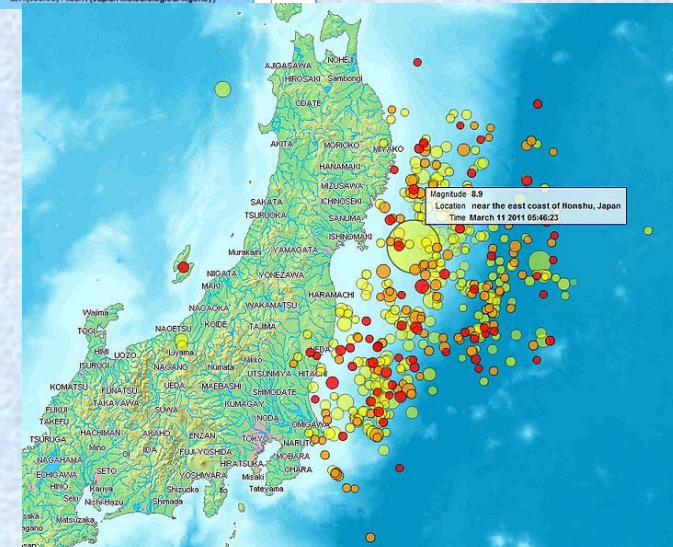
Tohoku-Oki Earthquake 2011

Occurred at 100 km off Sendai on 2:46PM 3.11 2011, M9.0, World 4th largest Earthquake

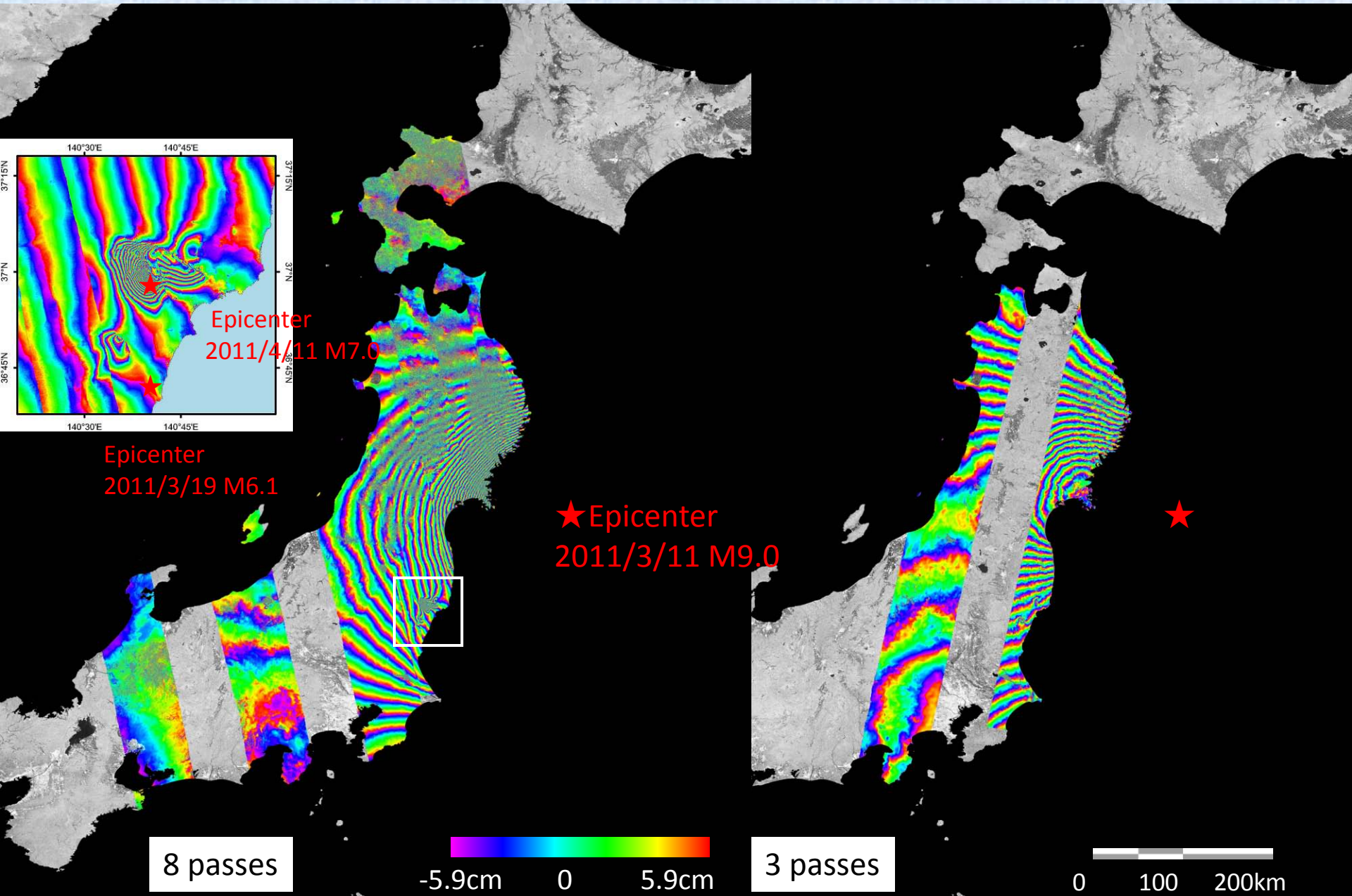
Dead: 15544
Missing: 5383
(July 10 2011)

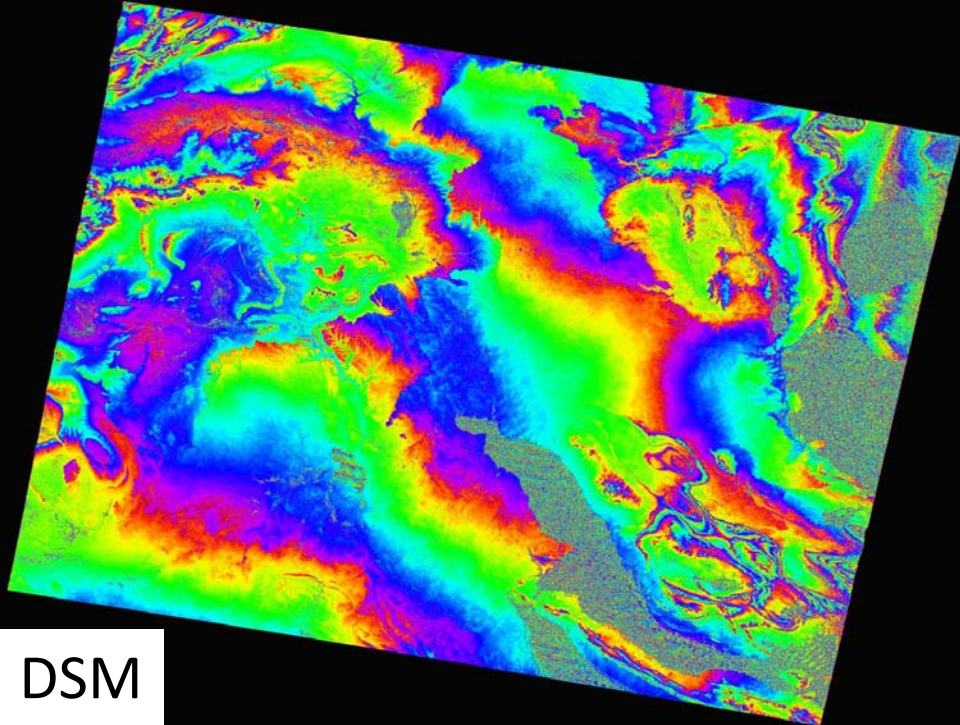


Seismic Intensity

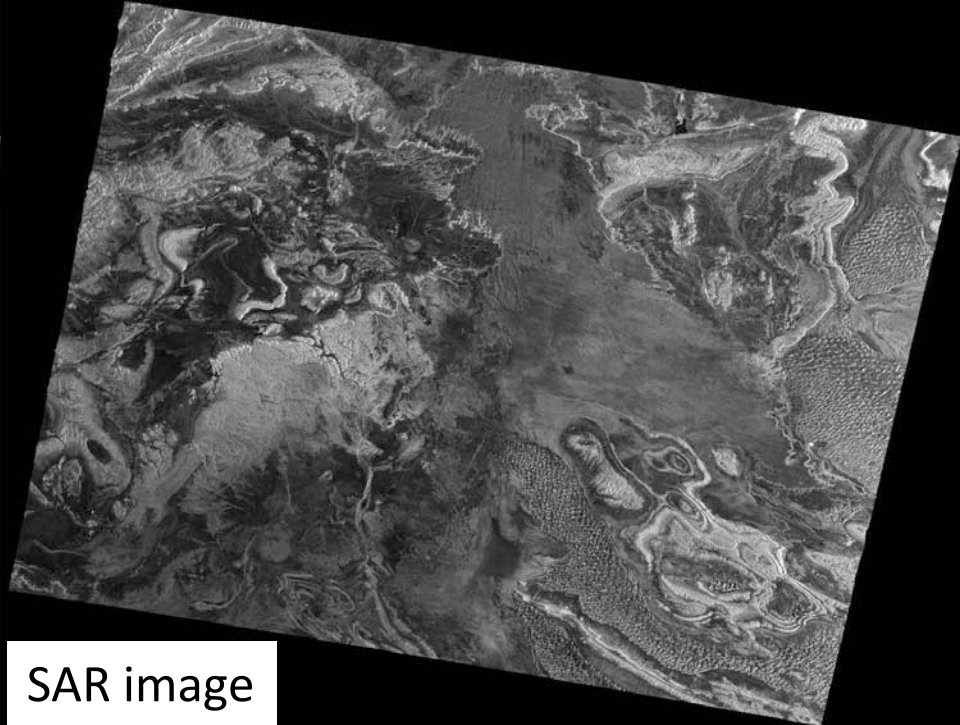


PALSAR DinSAR for Tohoku-Oki Earthquake





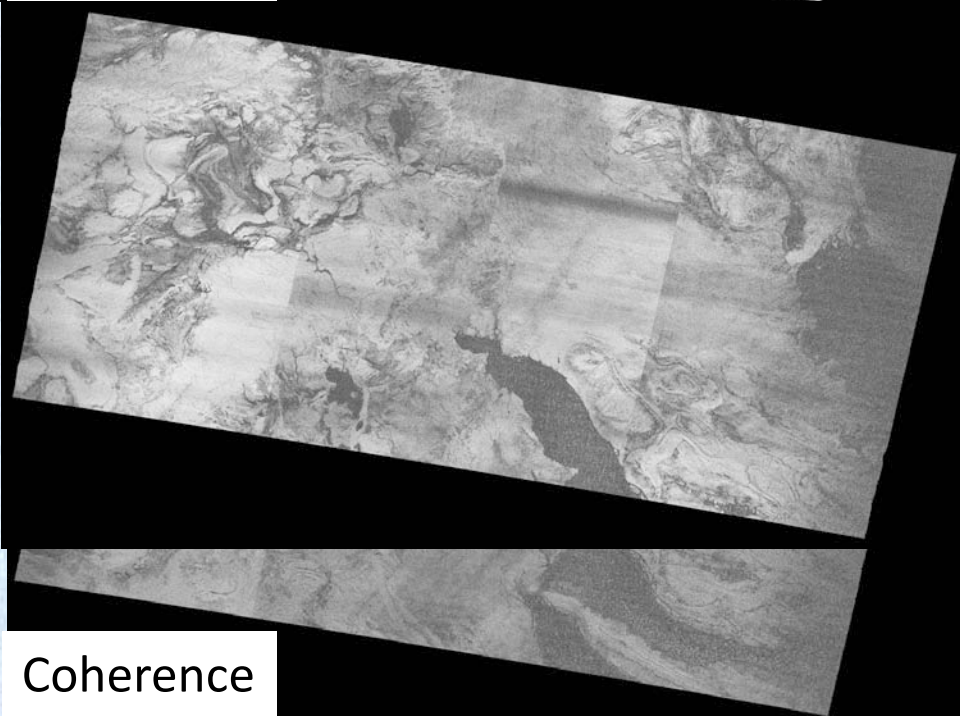
DSM



SAR image

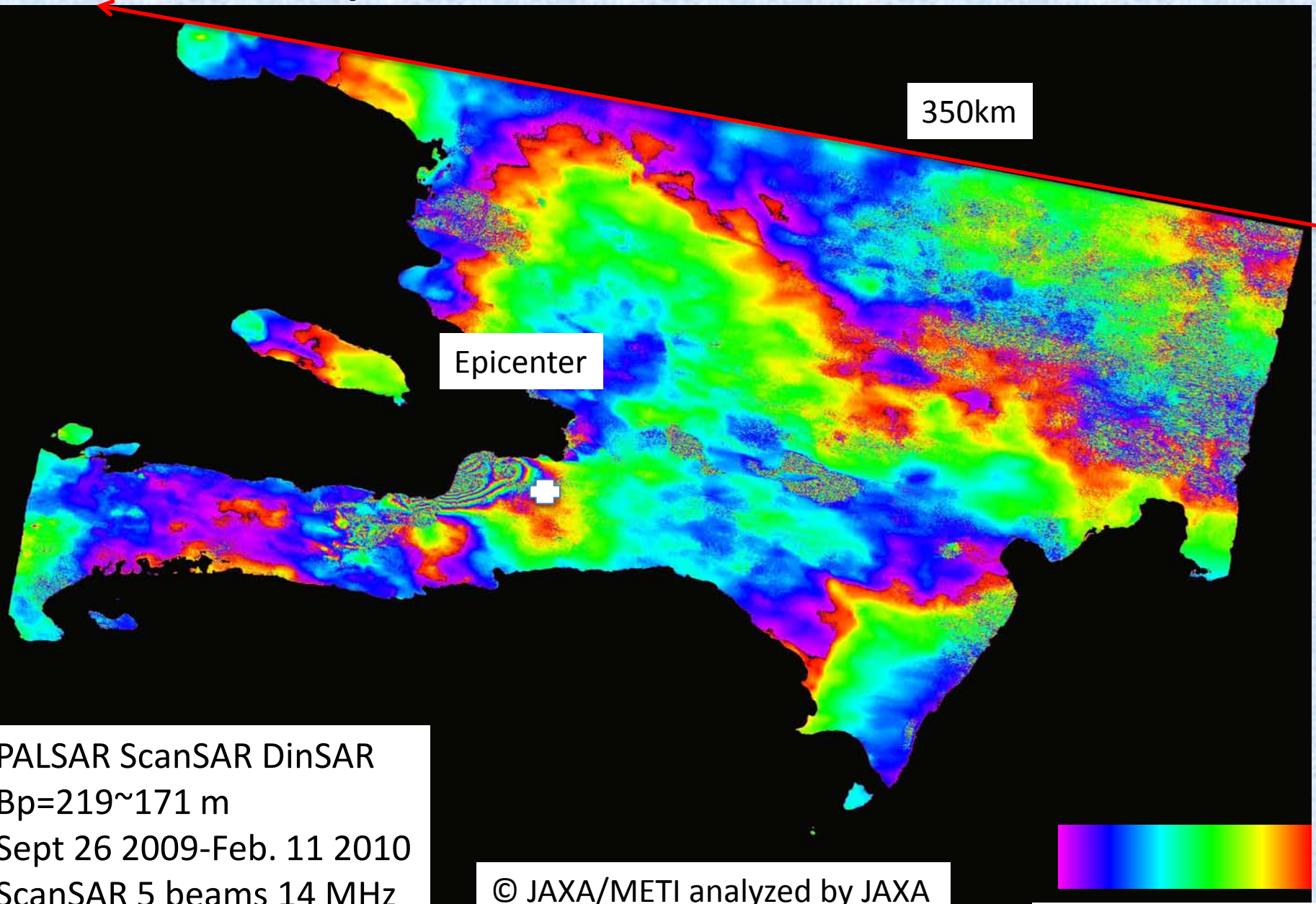
ScanSAR-ScanSAR Interferometry

- High Coherence
- Wide image areas (350km)
- Saharan Dessert
- $B_p \sim 200\text{m}$
- April 17 ~ March 4, 2008



Coherence

Haiti Earthquake (ハイチ地震: 精密軌道)



350km

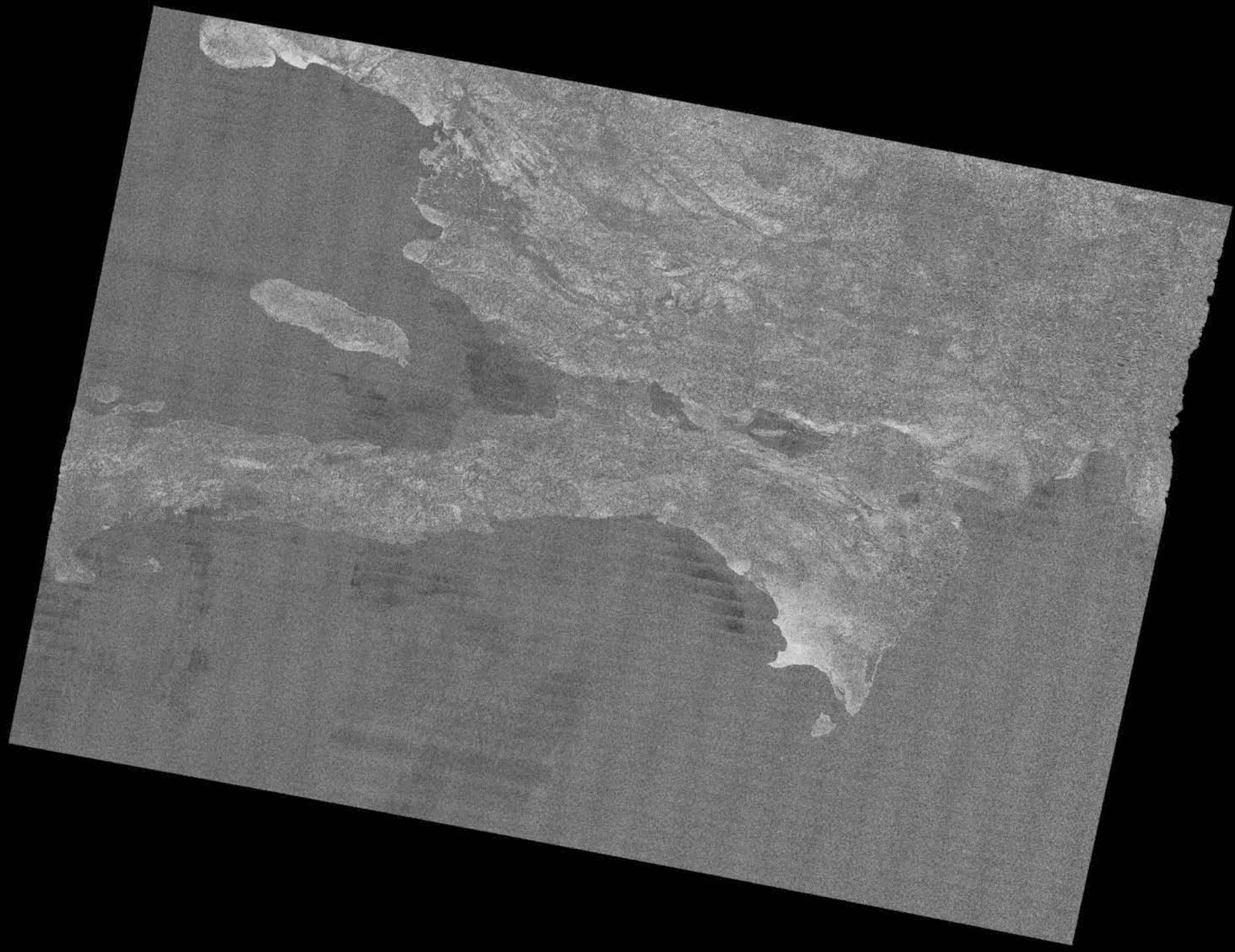
Epicenter

PALSAR ScanSAR DinSAR
Bp=219~171 m
Sept 26 2009-Feb. 11 2010
ScanSAR 5 beams 14 MHz

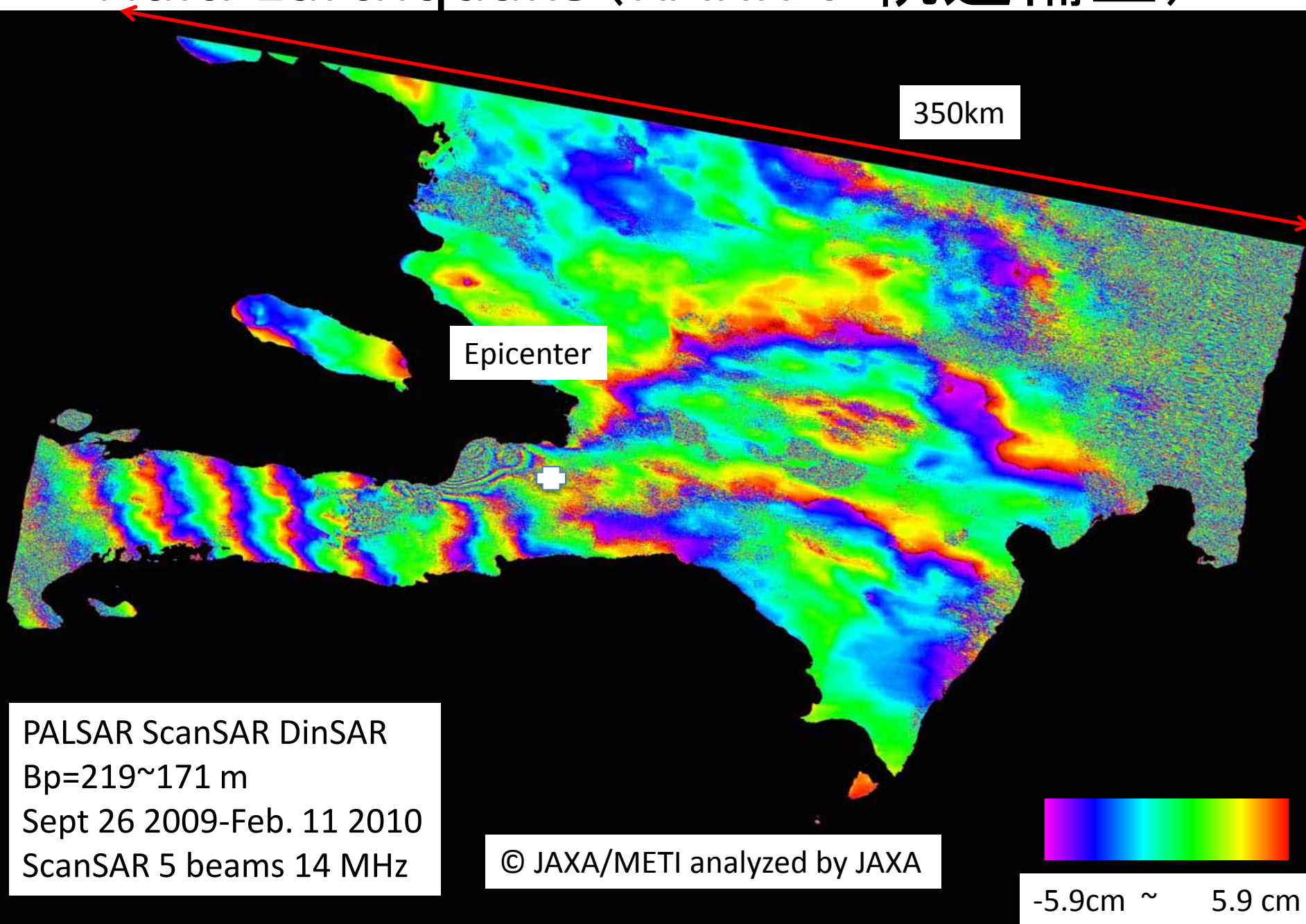
© JAXA/METI analyzed by JAXA



-5.9cm ~ 5.9 cm

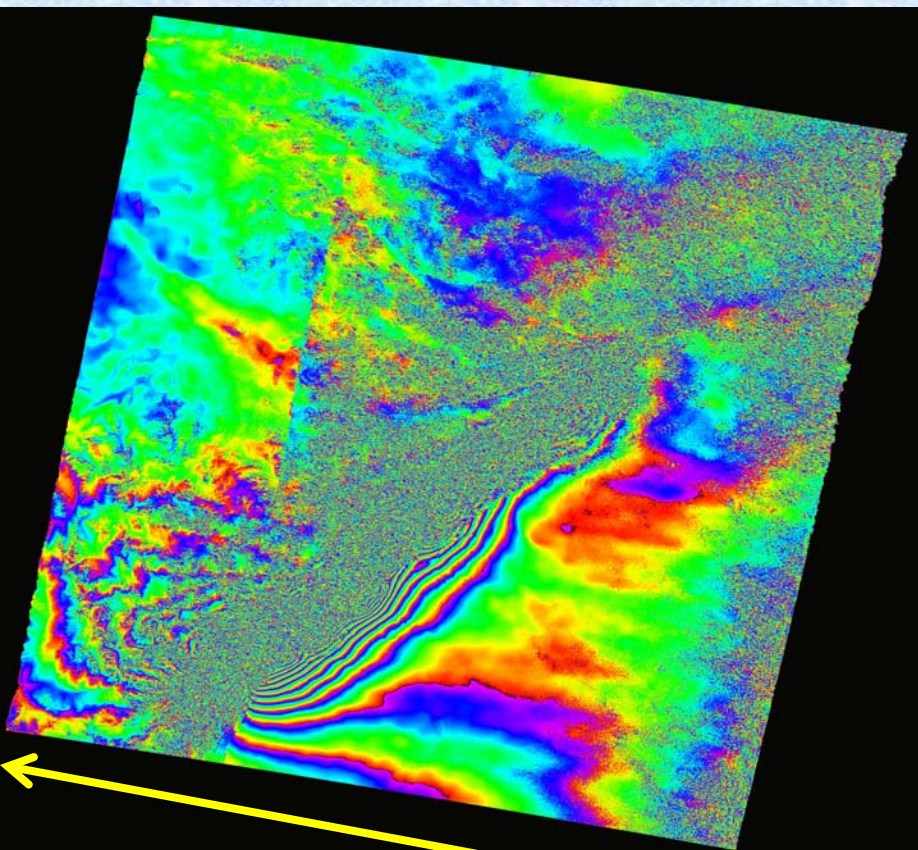


Haiti Earthquake (RARR + 軌道補正)

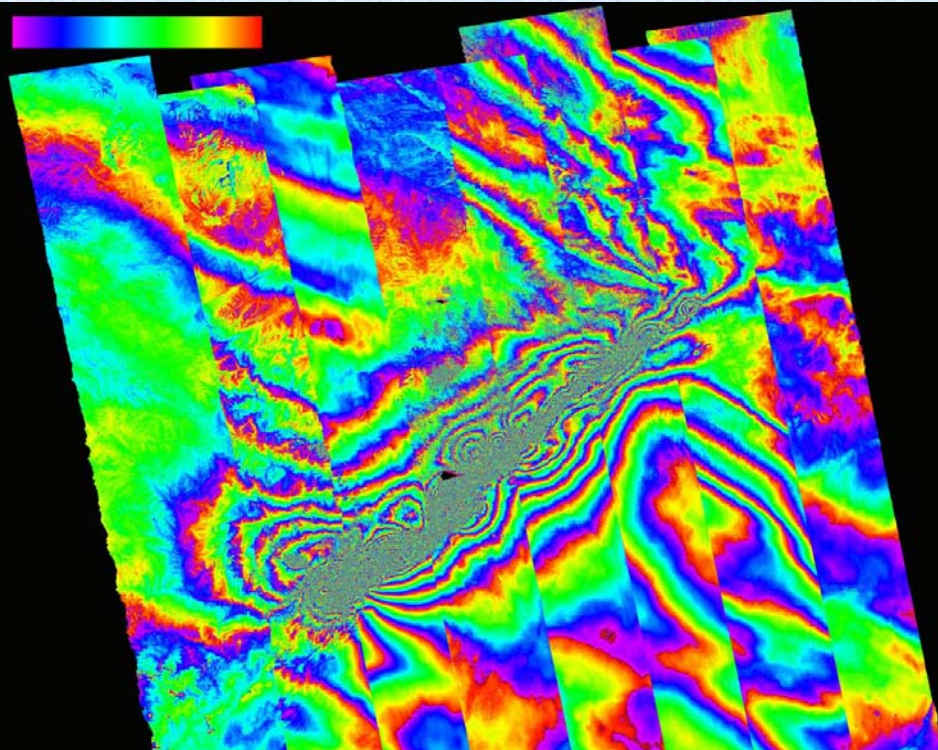


四川省大地震、2008年5月12日

ScanInSAR

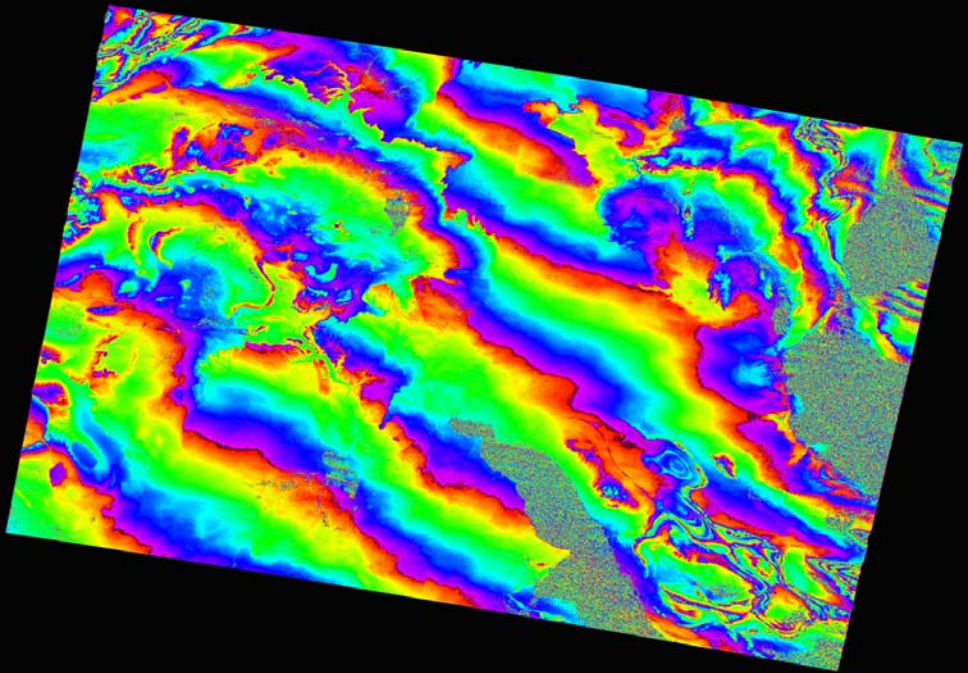
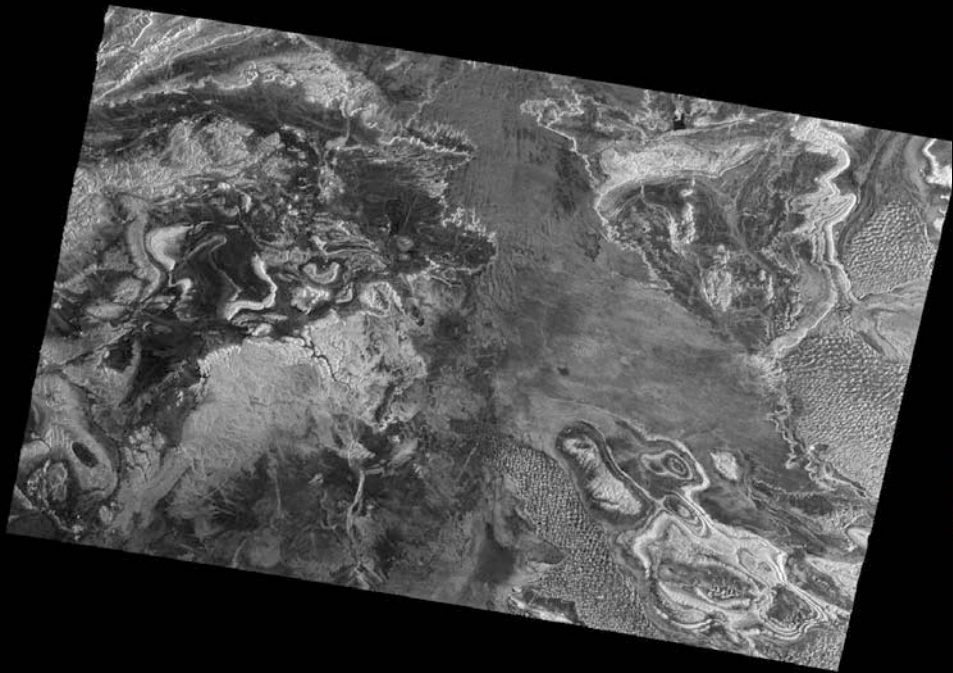
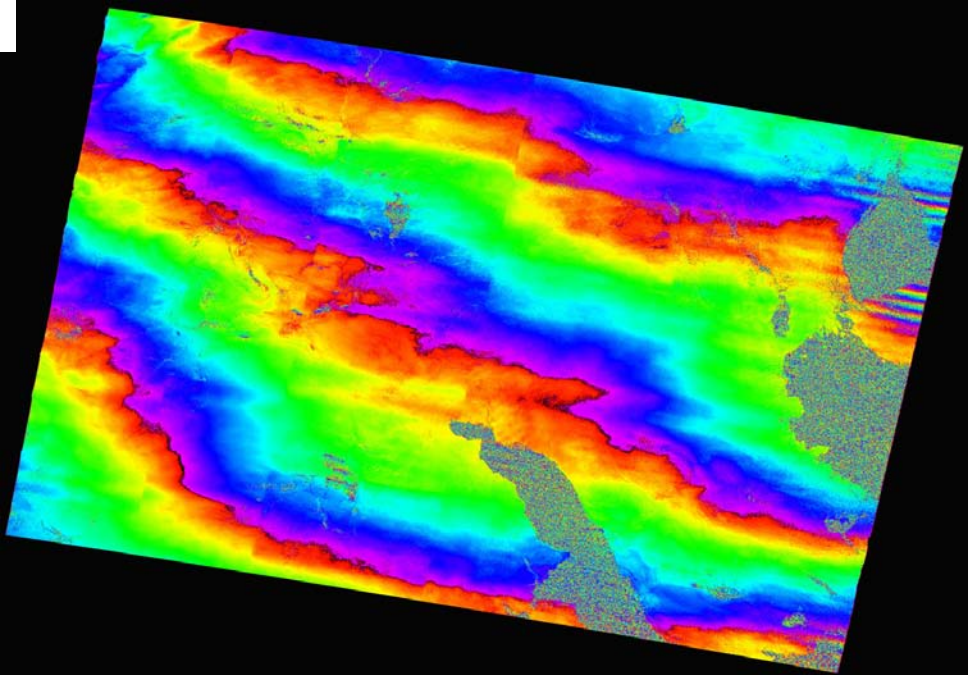
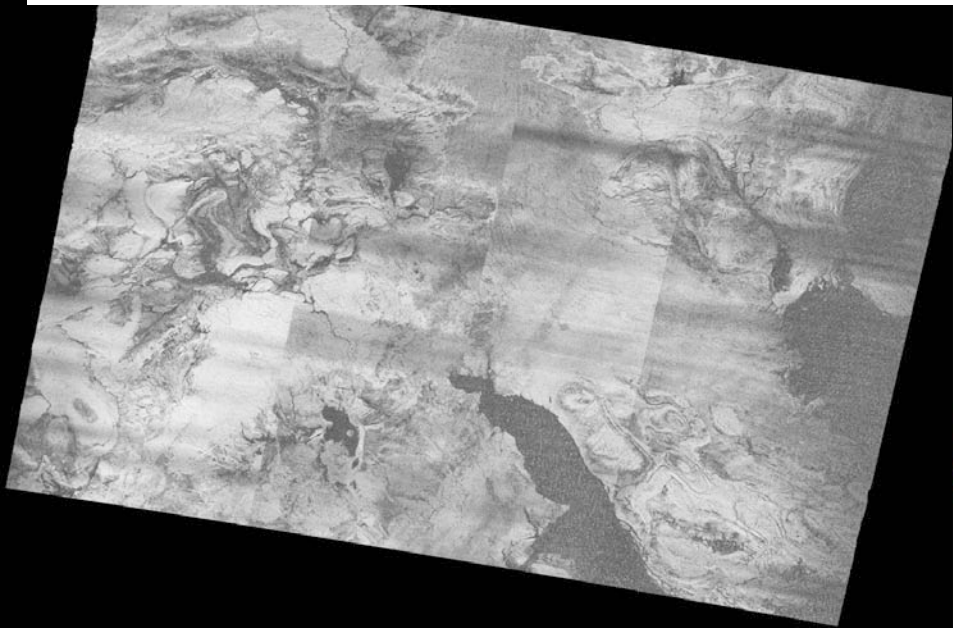


Strip SAR x 8

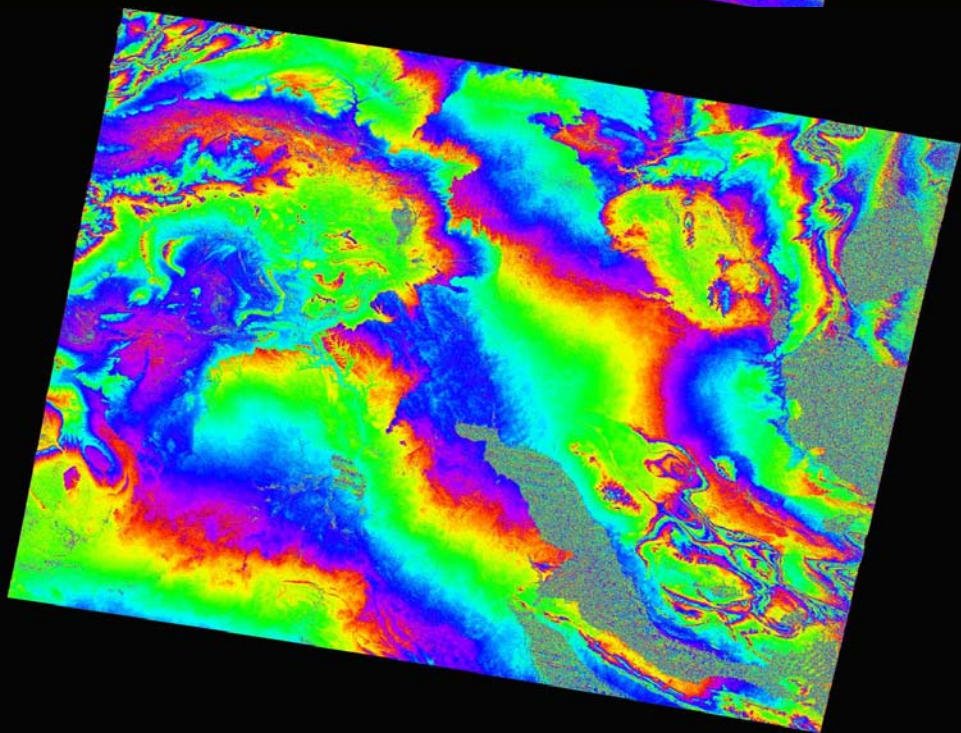
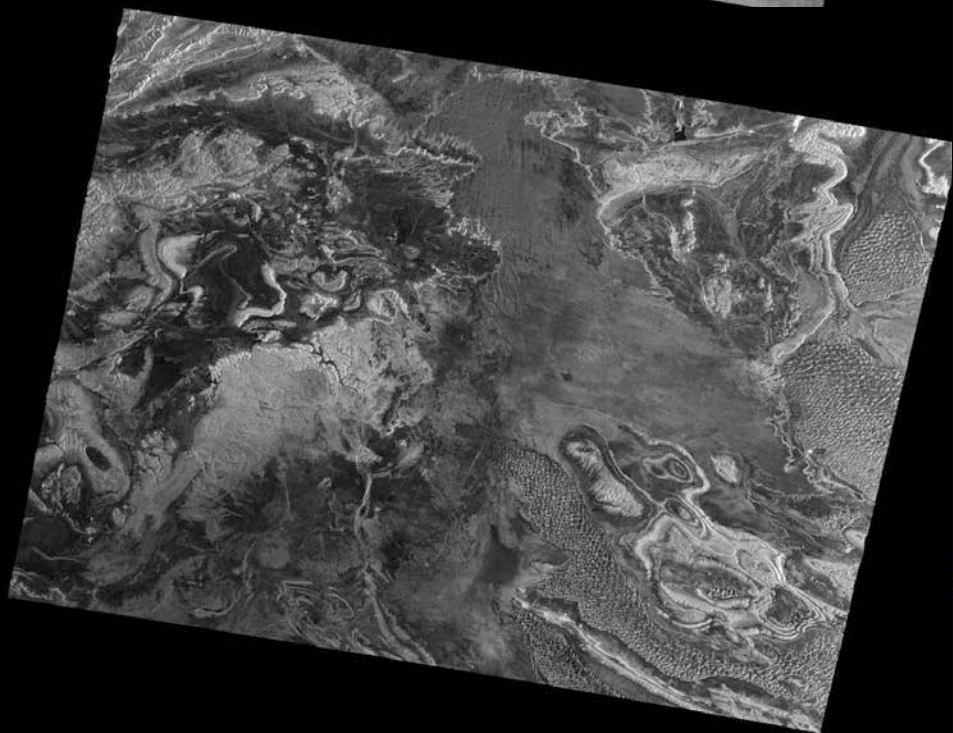
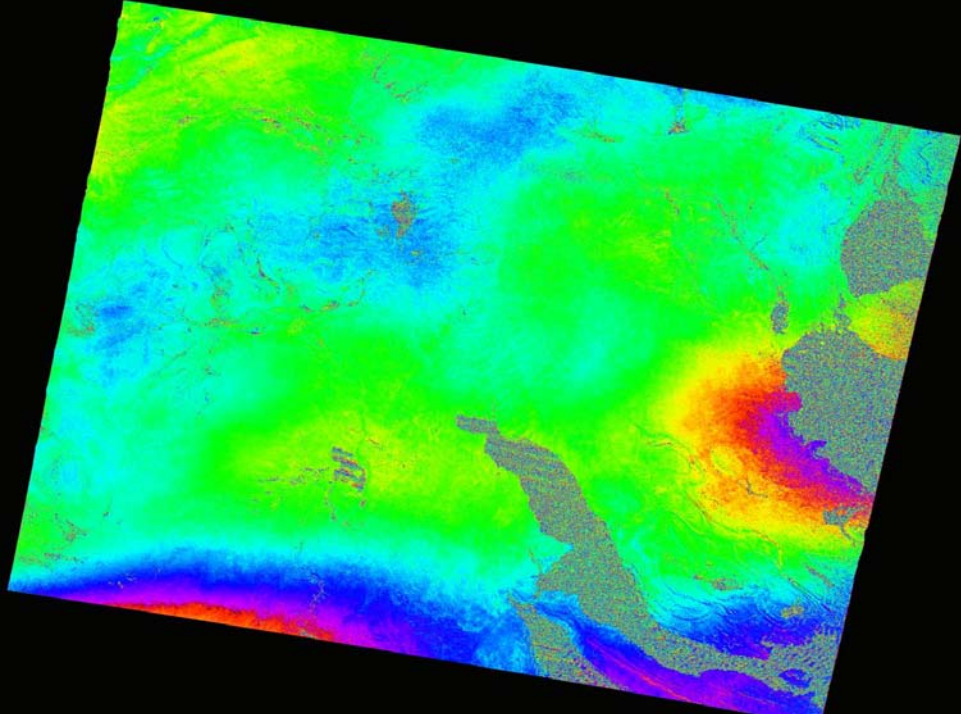
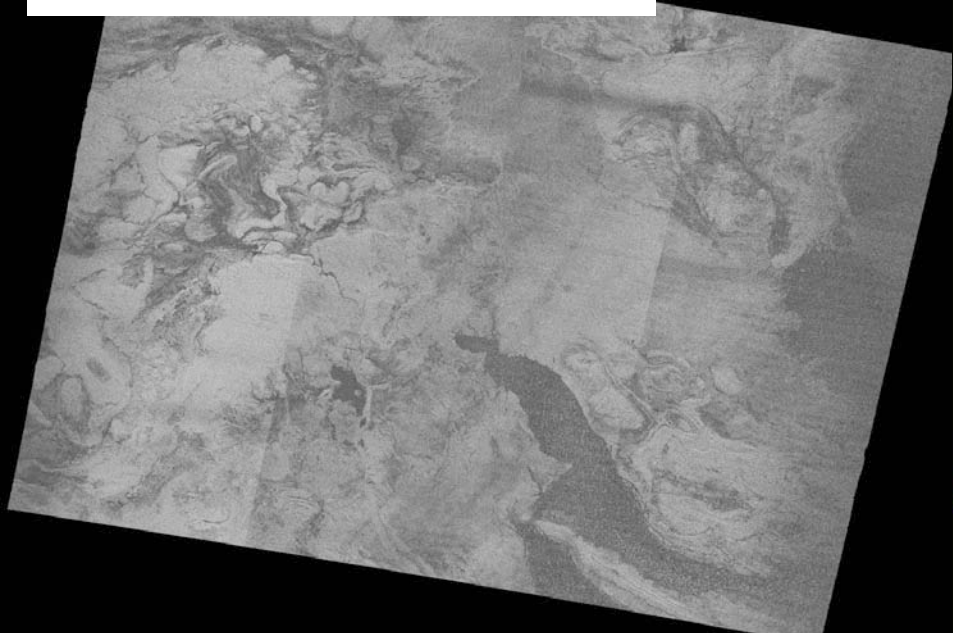


350km

タンザニア: コヒーレンス最大化処理を実施



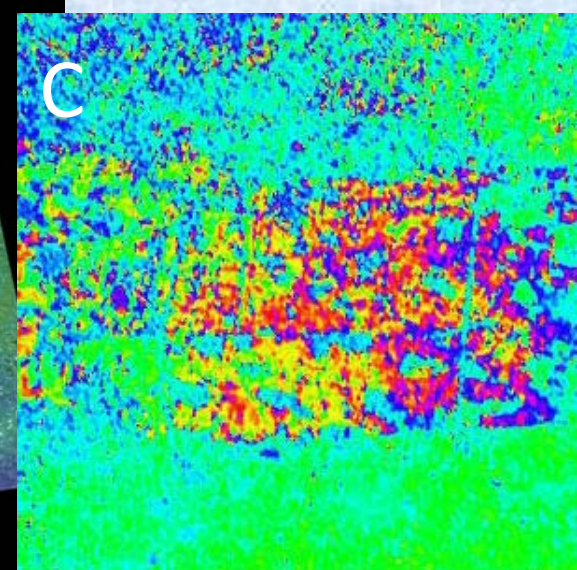
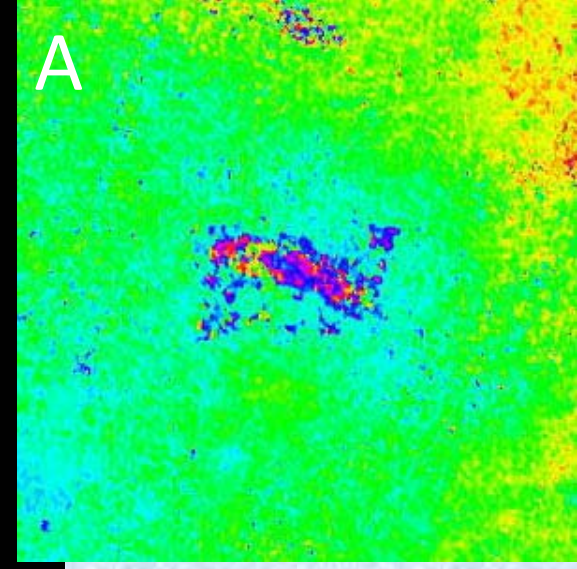
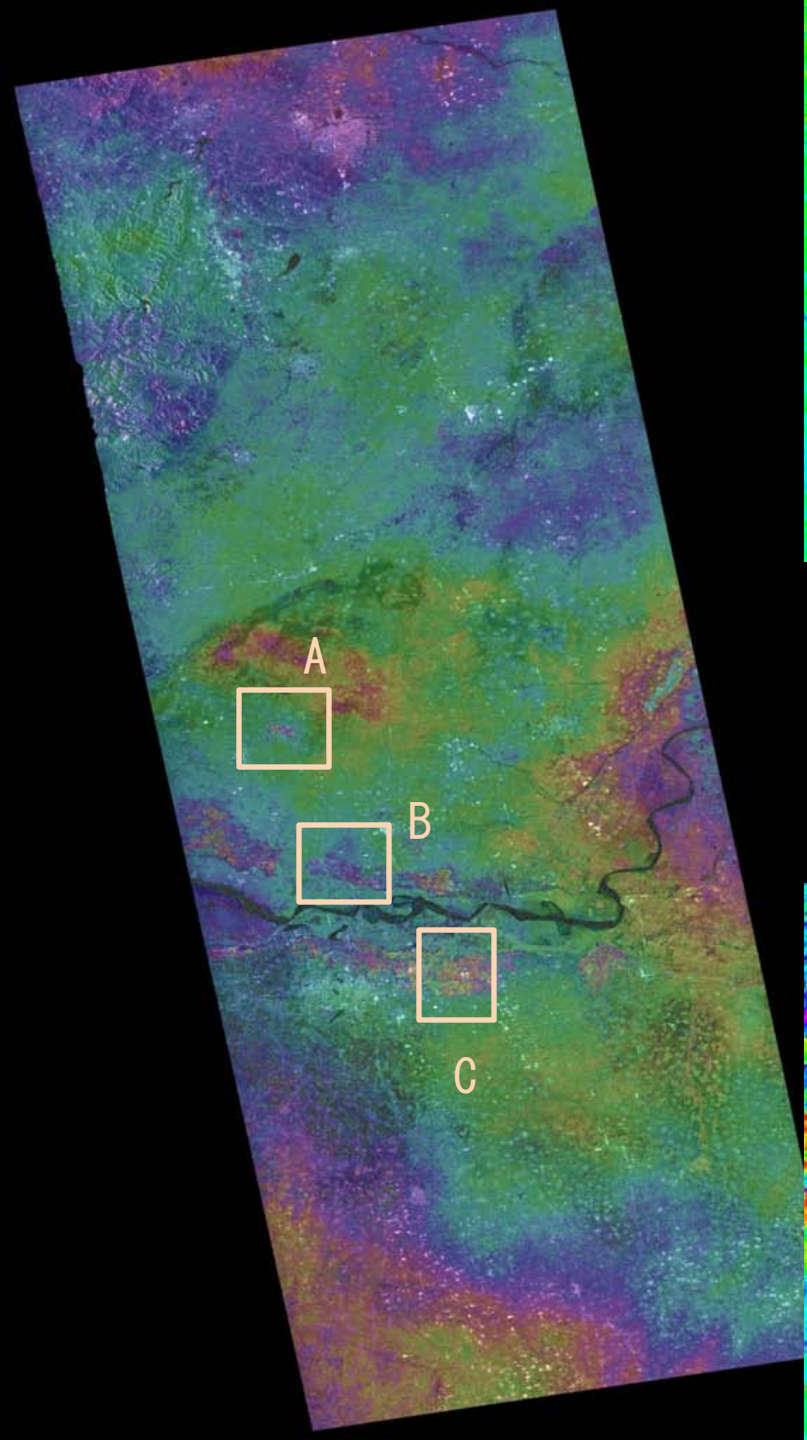
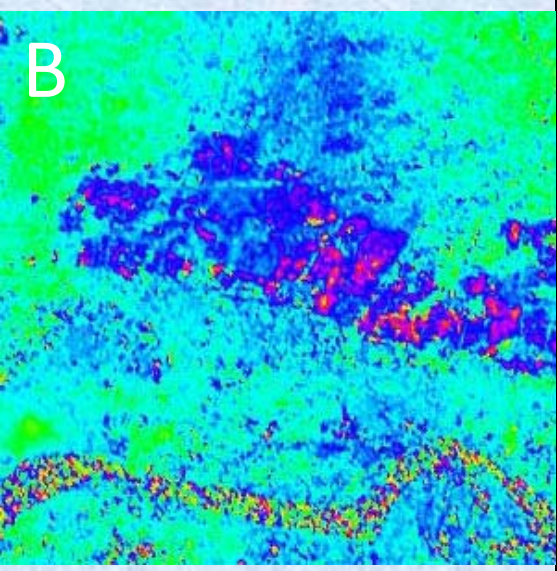
タンザニア: 疑似アフィン変換



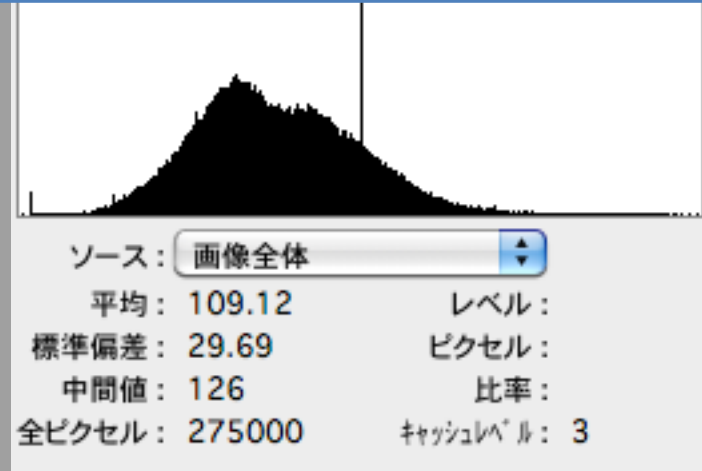
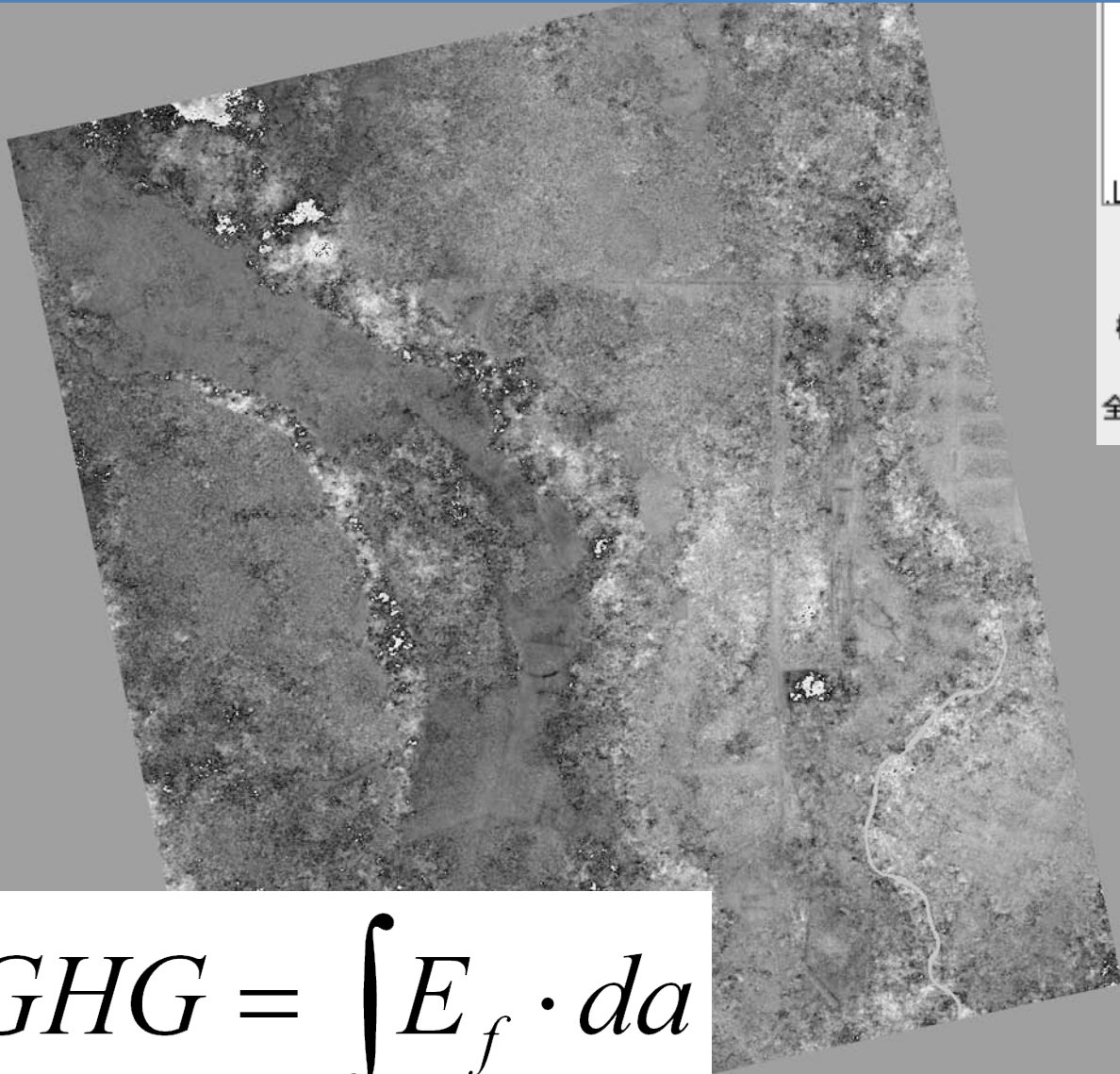
Drought and related subsidence around Yellow river, China

Master: FBS343H
2007/09/14
Slave : FBD343H
2007/07/30

Orb Distance: 110m



Subsidence and GHG emission at Central Kalimantan

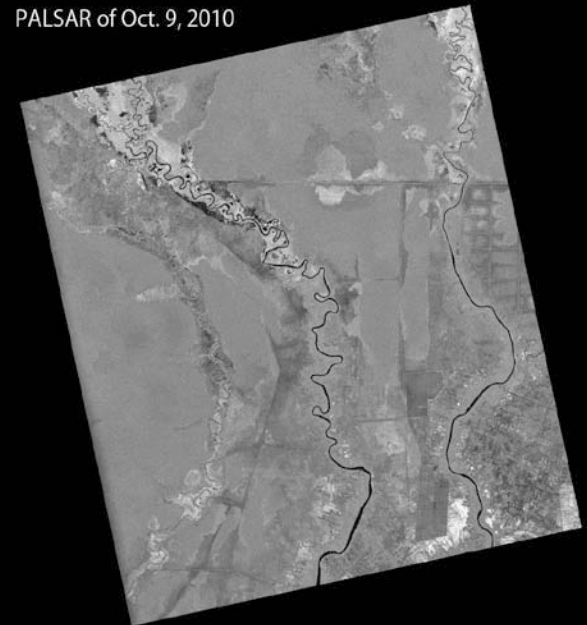


mean-subsidence=
-3.030946e+00 cm/year

$$GHG = \int E_f \cdot da$$

=13.0 MTonC

PALSAR of Oct. 9, 2010

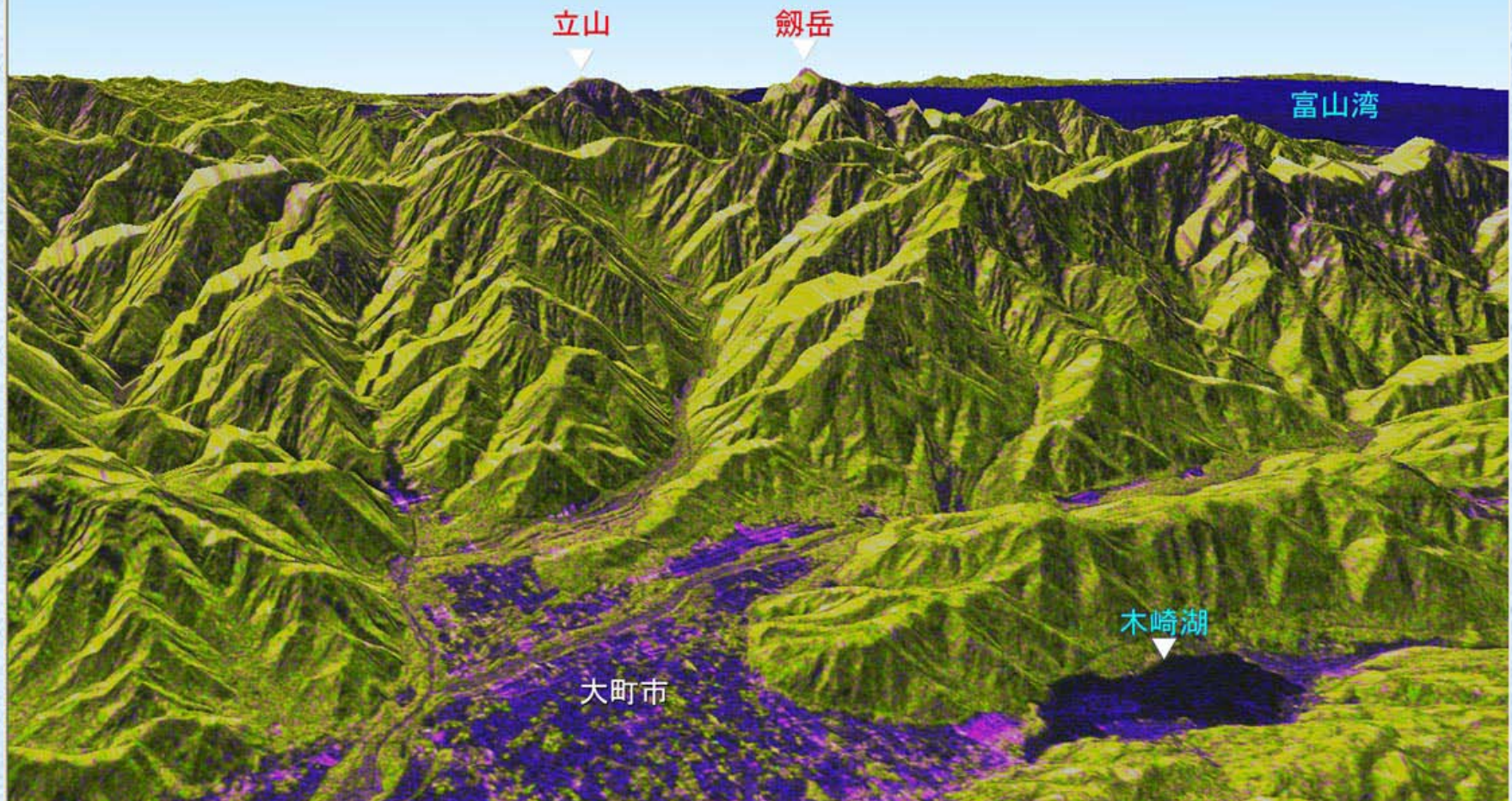


-12.8cm

12.8cm

PALSAR InSAR DEM

干渉SAR DEMの作成に関しては、46日以上を繰り返す干渉のために気象の影響を受ける。そのために、5ペア以上を相加平均して、誤差を小さくする。大山で評価して、30m以内の精度を確認した。本例は、富山県剣岳周辺のDEMを作成し、FBD画像を重ねあわせ、立体視したものである。2007年の生産数は5.4シーン／日であり、仕様を満足している。



InSAR Sensitivity – L band

- Incidence angle dependence
- Seasonality
- Ionosphere (TID and Plasma Bubble)
- Orbit Accuracy and Statistics
- Multi Frequency Comparison
- Comparison between JERS-1 and PALSAR

Coherence analysis: Temporal correlation

$$\gamma_{total} = \frac{|\langle a \cdot b^* \rangle|}{\sqrt{\langle a \cdot a^* \rangle \langle b \cdot b^* \rangle}} \quad \longrightarrow \quad \gamma_{temp} = \frac{\gamma_{total}}{\gamma_{SNR} \cdot \gamma_{space} \cdot \gamma_{vol}}$$

$$= \gamma_{temp} \cdot \gamma_{space} \cdot \gamma_{SNR} \cdot \gamma_{vol}$$

$$\gamma_{vol} \leq \text{sinc}(k_z h_v / 2)$$

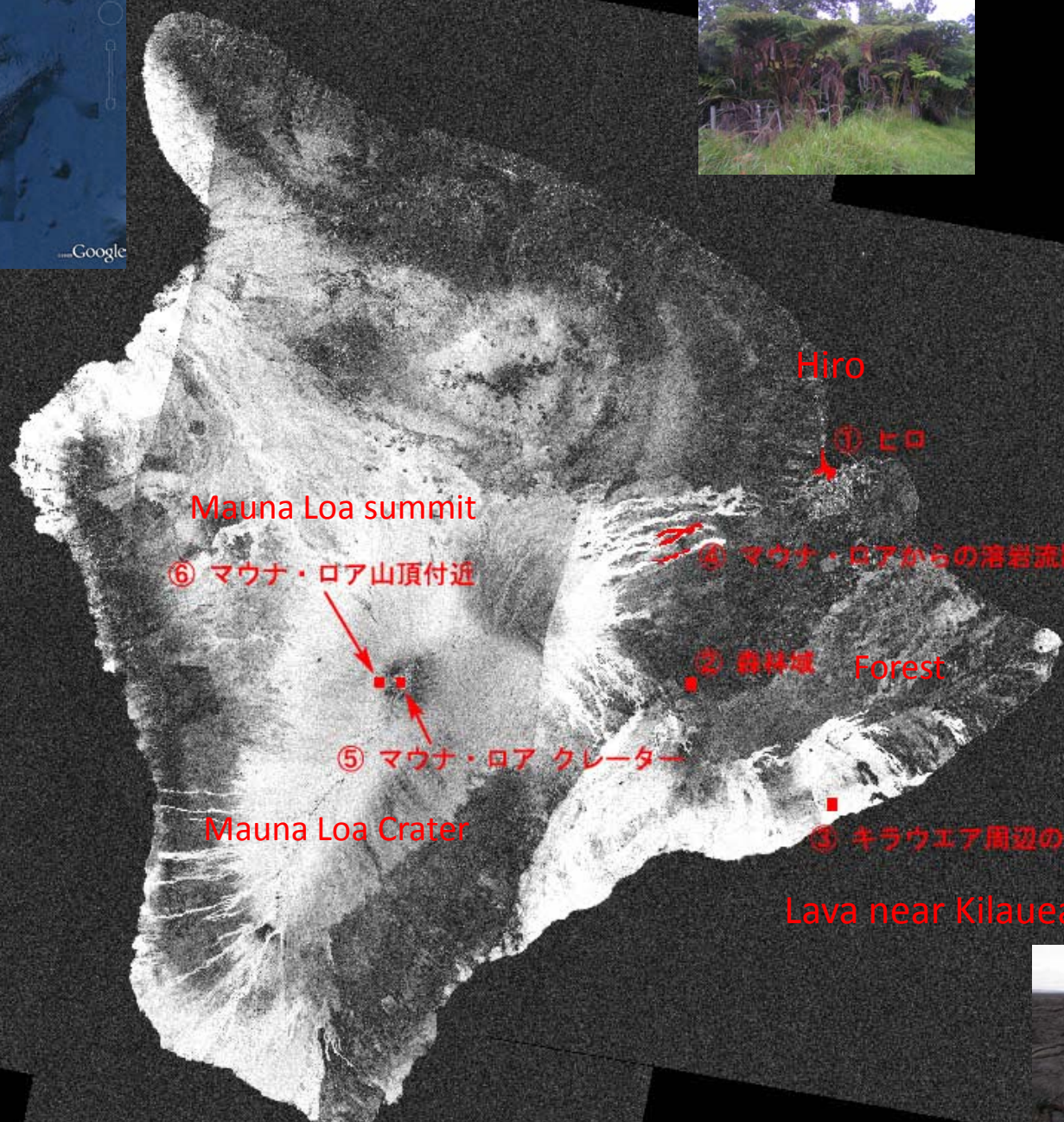
$$\gamma_{space} \approx 1 - \frac{2|B| \cos^2 \theta}{\lambda r} \frac{c}{B_w \sin \theta}$$

$$\gamma_{SNR} = \frac{1}{1 + SNR^{-1}}$$

kz: the sensitivity of interferometric phase to height, hv: ambiguous volume height

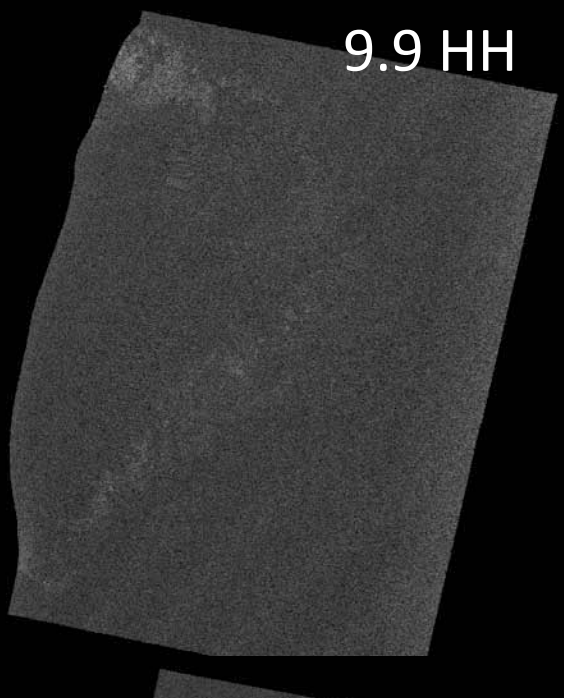
θ : incidence angle, B_w : Band width
 r : slant range, B : baseline

γ_{SNR}	σ^0	σ^0_{NE}	sensor
~0.9	-5~-10 dB	-18 dB	JERS-1
1.0	-8 ~ -15 dB	-25 dB	PI-SAR
1.0	-8~-15dB	-27~-34dB	PALSAR

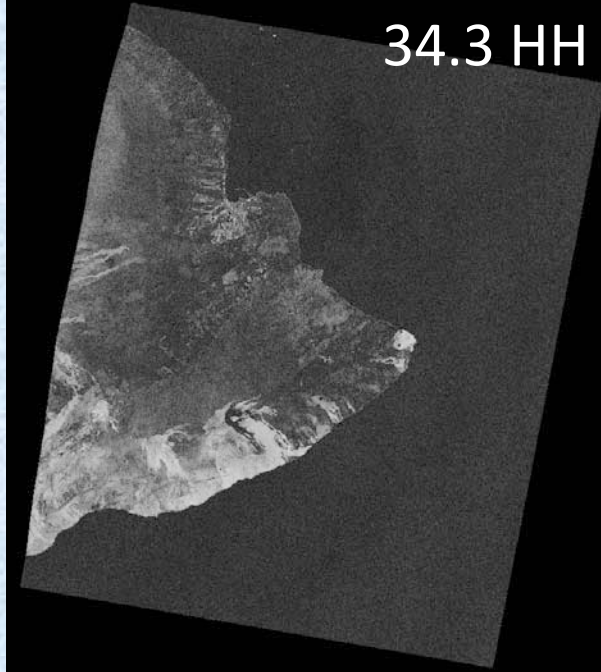


Coherence map of the Hawaii island

9.9 HH

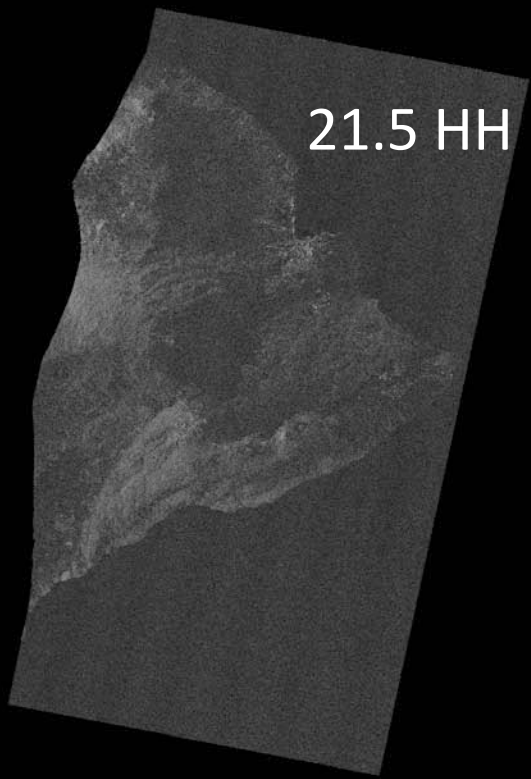


34.3 HH

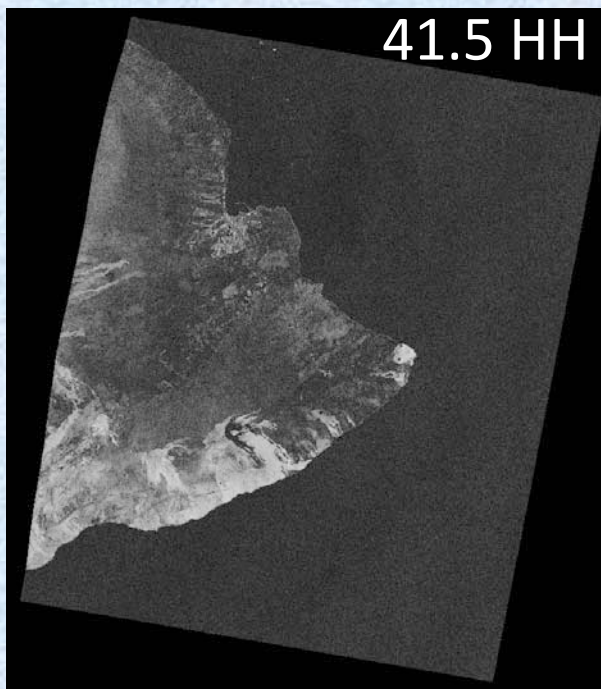


Comparison of
coherence WRT
off-nadir angle

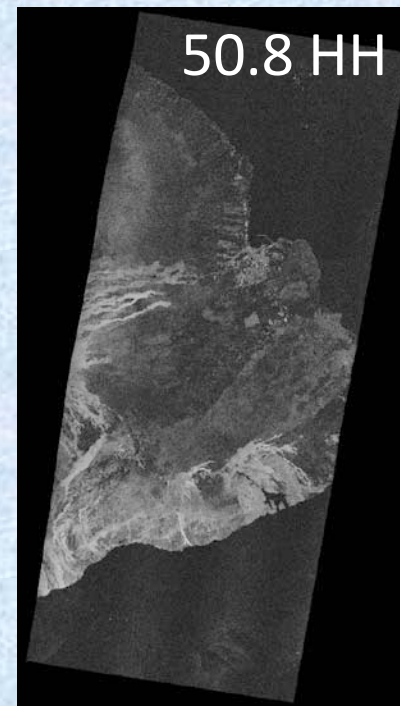
21.5 HH



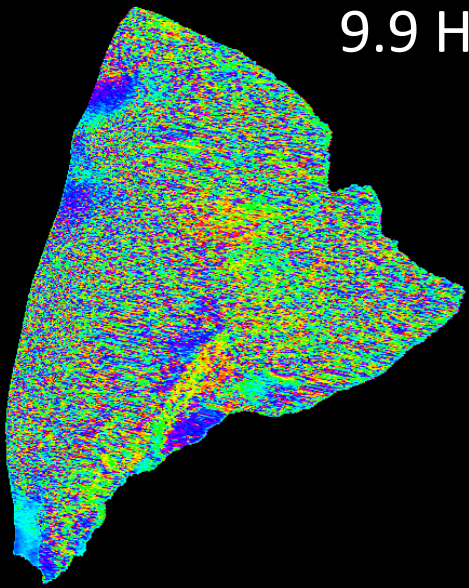
41.5 HH



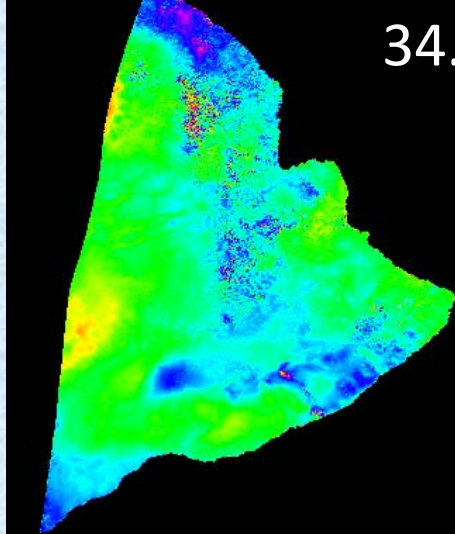
50.8 HH



9.9 HH

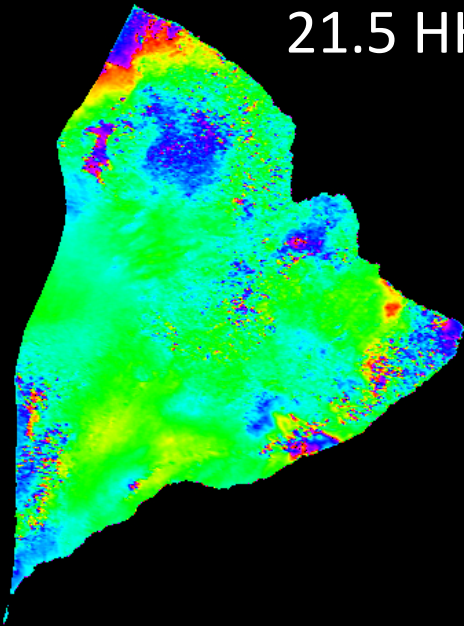


34.3 HH

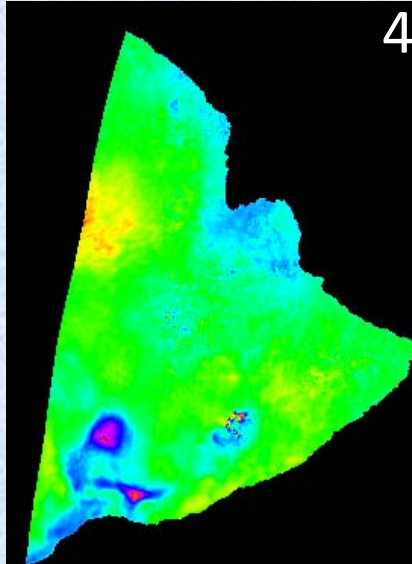


Comparison of
DinSAR WRT off-
nadir angle

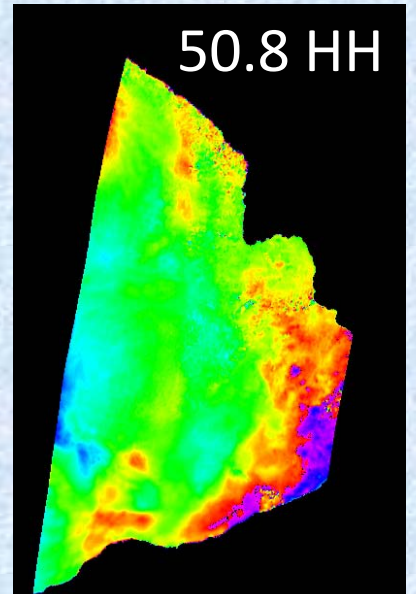
21.5 HH



41.5 HH



50.8 HH



Incidence angle dependence of coherence

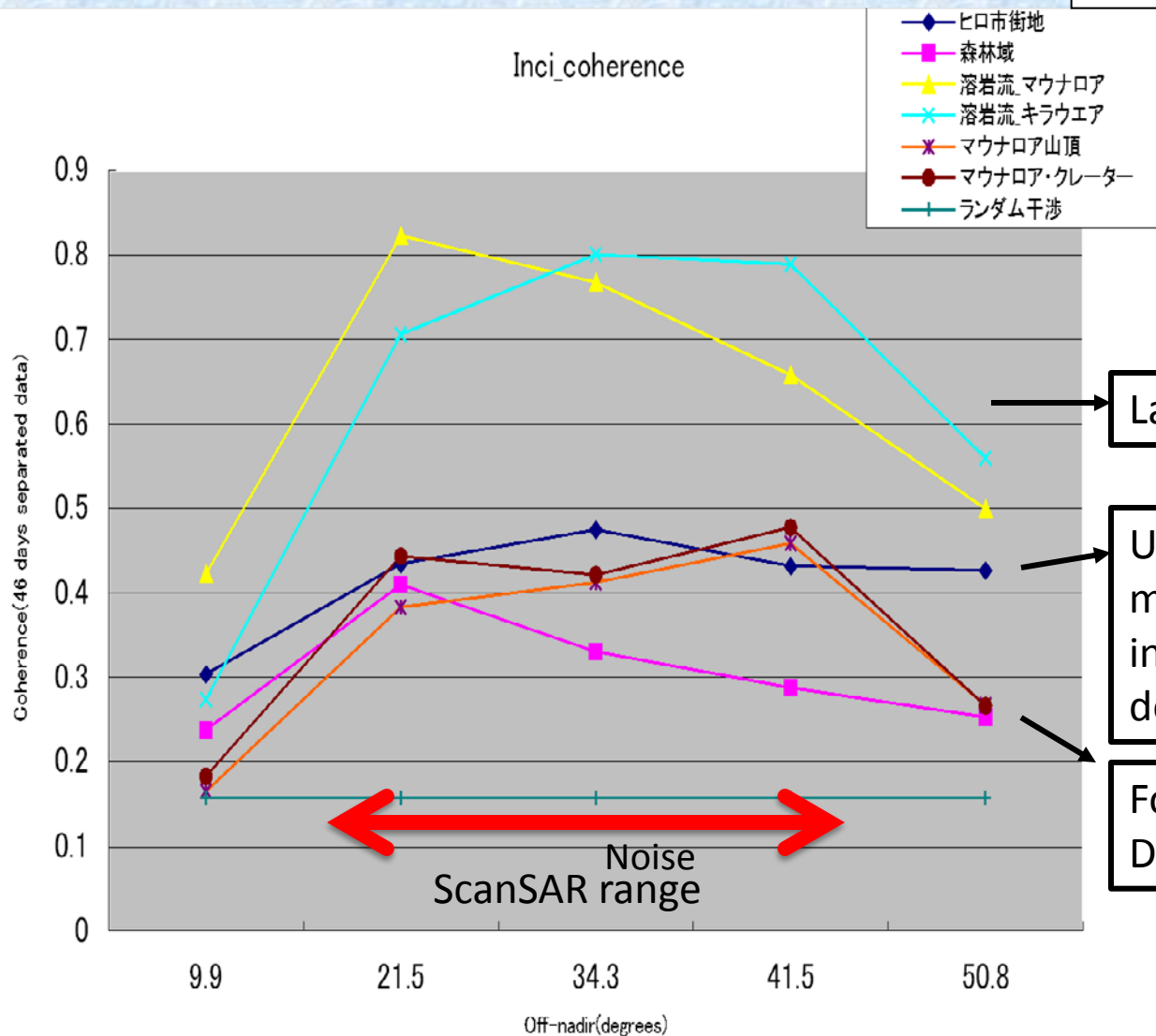
Condition:

Only 46 days separated data used.

No-temporal correlation corrected

Bp:~200m

No. of data ~ 2,3.



Lava: shows high coherence

Urban and volcanic mountain :increase with the incidence angle by 41.5, then decreases.

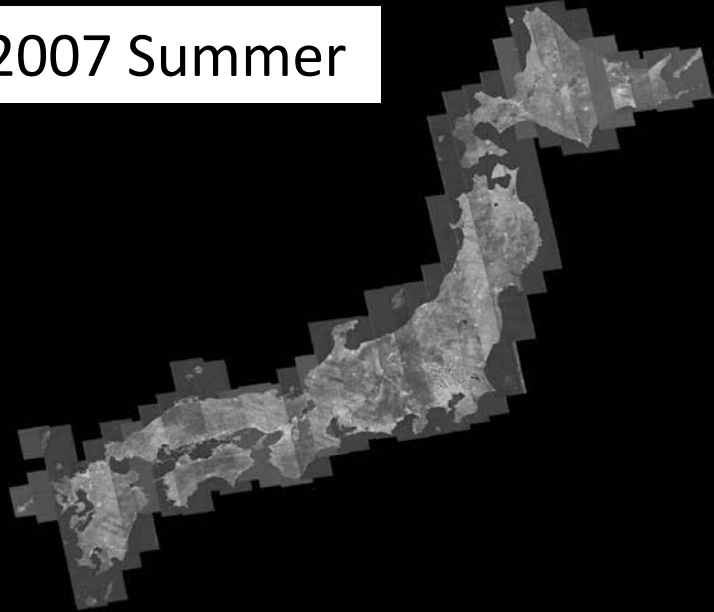
Forest: maximized at 21.5. Decreased after the angle.

Type A: Others
Type B: Forest

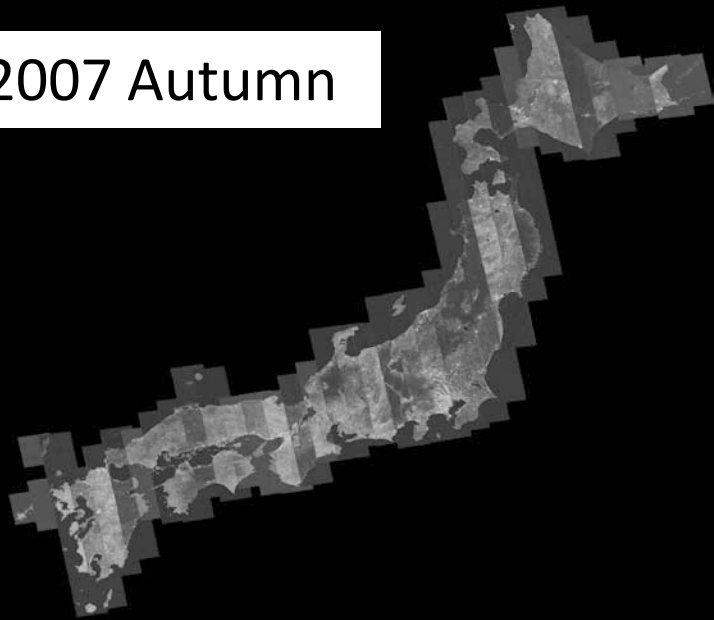
PALSAR InSAR coherence WRT Season

- SAR Processor: SIGMA-SAR
- Total Data : 500GB : Two sets of 41 passes covering Japan (2007 summer, 2007 autumn, 2007 winter, and 2008 spring)
- Precise Orbit: (40 cm: 3 sigma)
- Evaluation Items
 - Coherence vs. season
 - Deformation Uniformity vs. season
 - Perpendicular Baseline Characteristics

2007 Summer

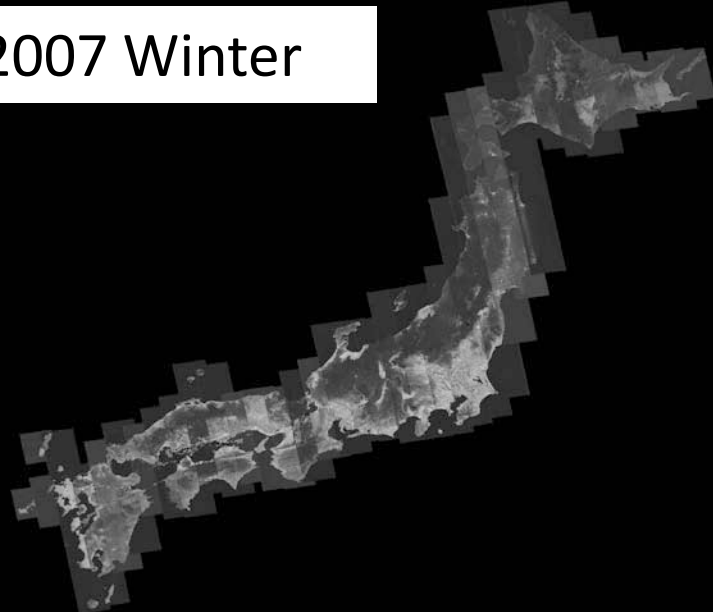


2007 Autumn

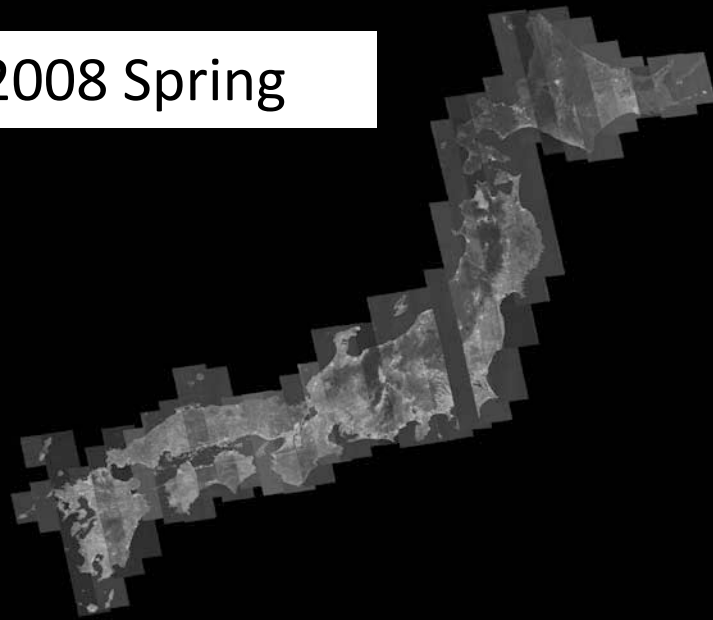


Autumn, 2007

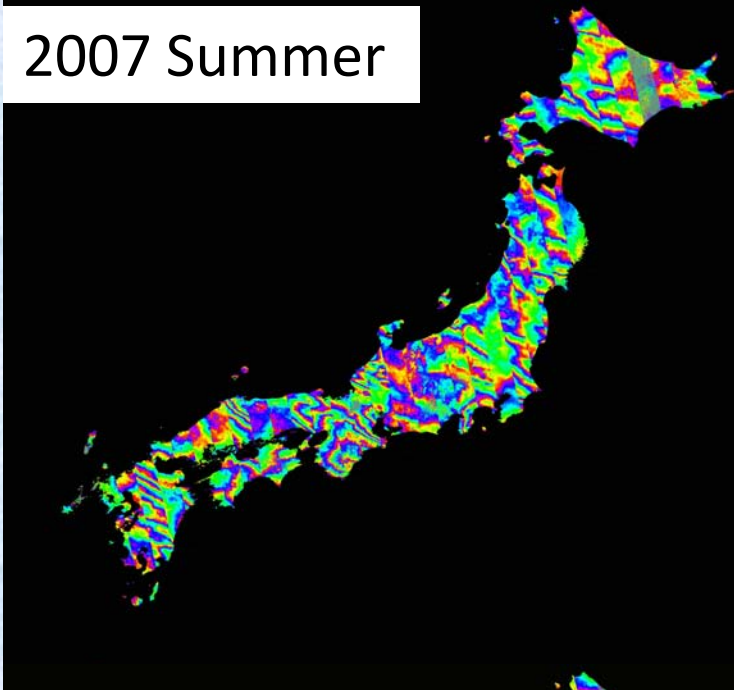
2007 Winter



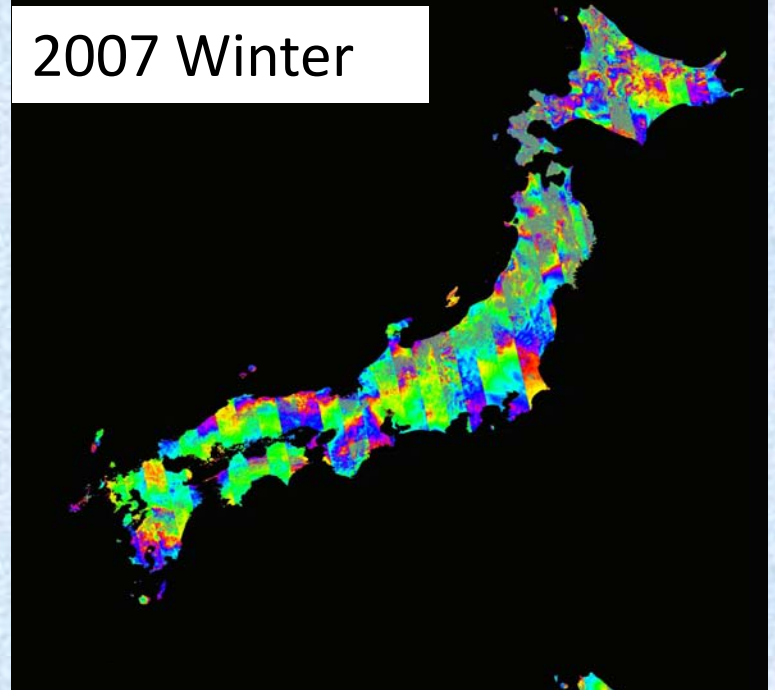
2008 Spring



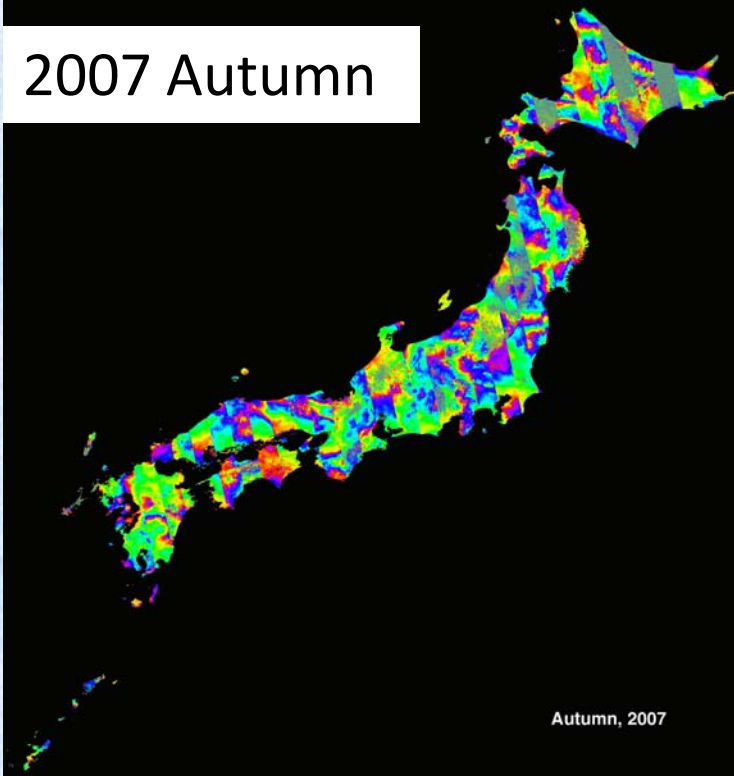
2007 Summer



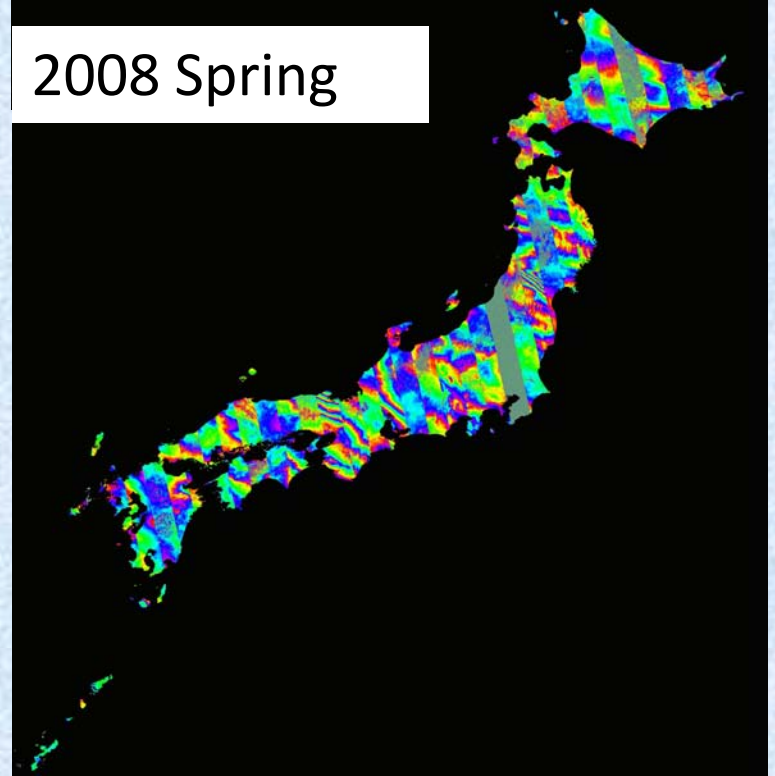
2007 Winter



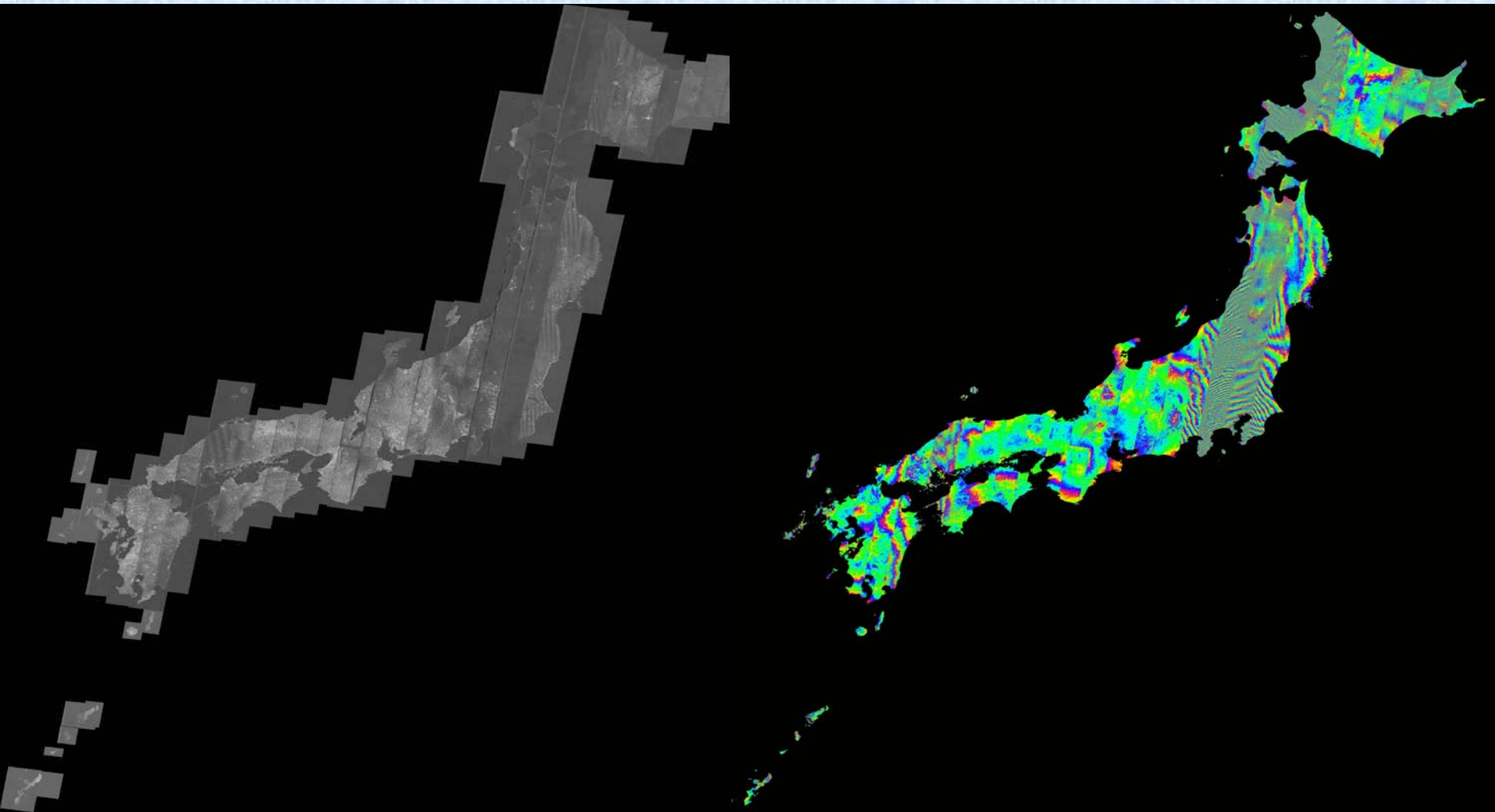
2007 Autumn



2008 Spring



JERS-1 SAR data



Summary

- Coherence:
- Summer > Winter (Mountain area lower values)
- Mountain area: lower than flat (larger band width)

- Phase deformation: Winter is more uniform than Summer
- Descending orbit is better than Ascending orbit

- Best selection: Winter and descending orbits

- Select a bit larger off-nadir for better coherence(ScanSAR beam selection)

Orbit determination

Orbit determination	Spec.	Measurements (* is after May 16 2006)		
Onboard determination (<95%) Quick distribution	< 200 m	35m	Random	23m (X: 8m, Y: 8m, Z: 20m, all 2σ)
			bias	12m (2σ)
GUTS-offline determination(3σ) Three days for distribution after observation	< 1m	0.40 m*	random	0.21m* (3σ) (Overlap method)
			bias	0.18m (3σ) (SLR ranging of Aug.)

Type of orbits

Range and range rate(Estimated)

Range and range rate(post processed)

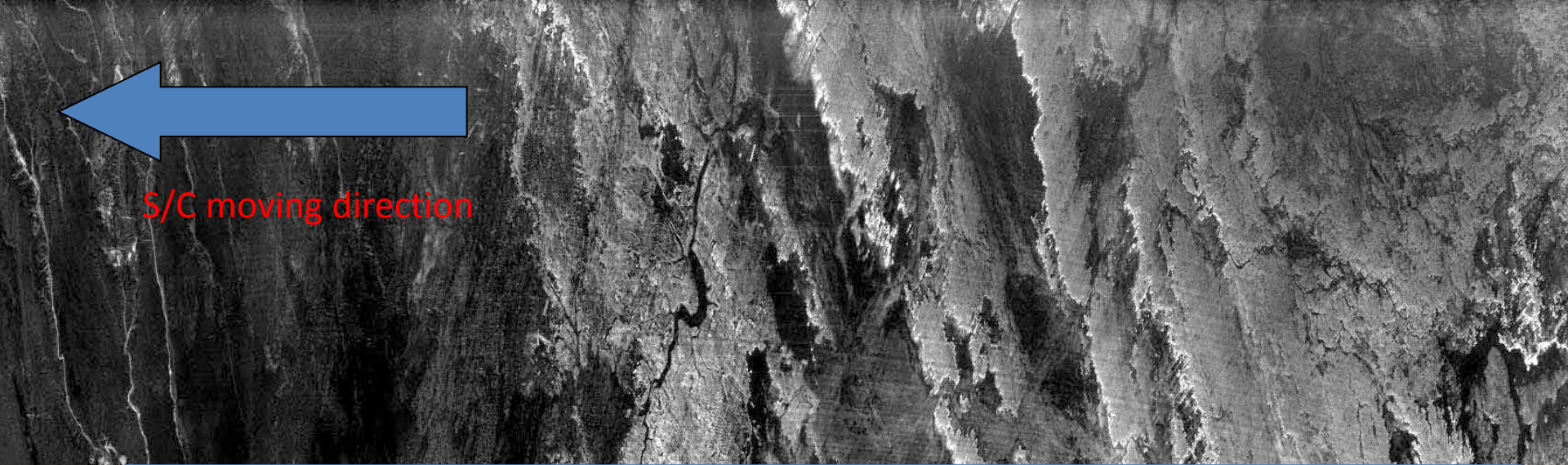
Onboard data

GUTS-off line data (Most accurate)

ECR(Earth Centered Rotational)

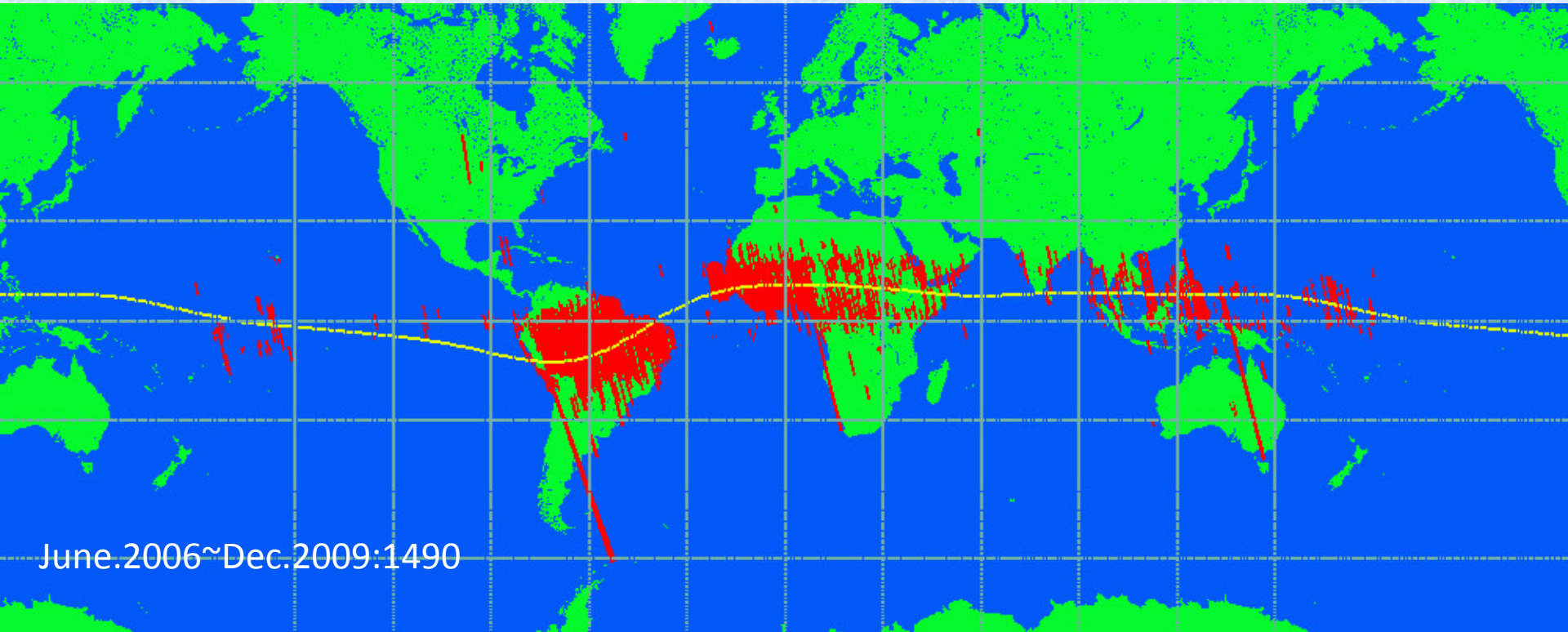


recommended



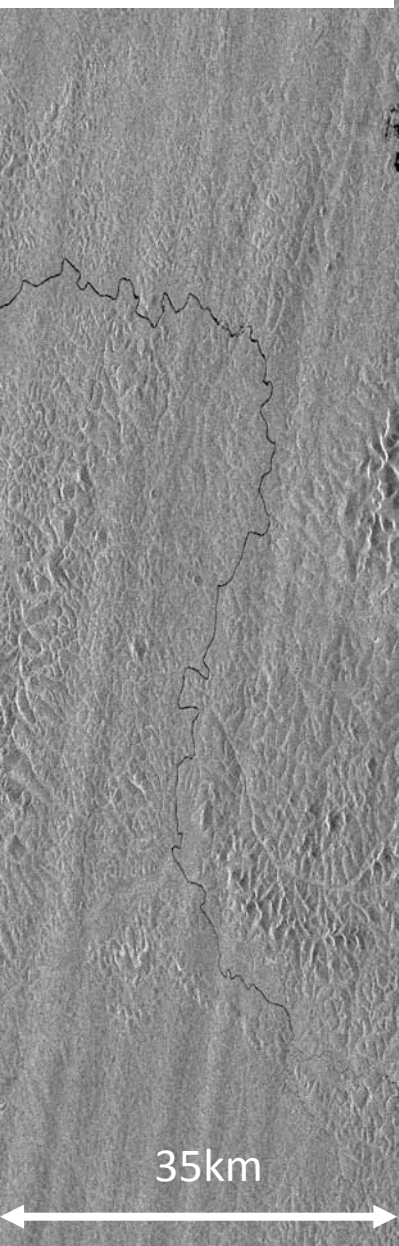
Plasma Bubble and the related PALSAR Images

PALSAR Streaks Appearance

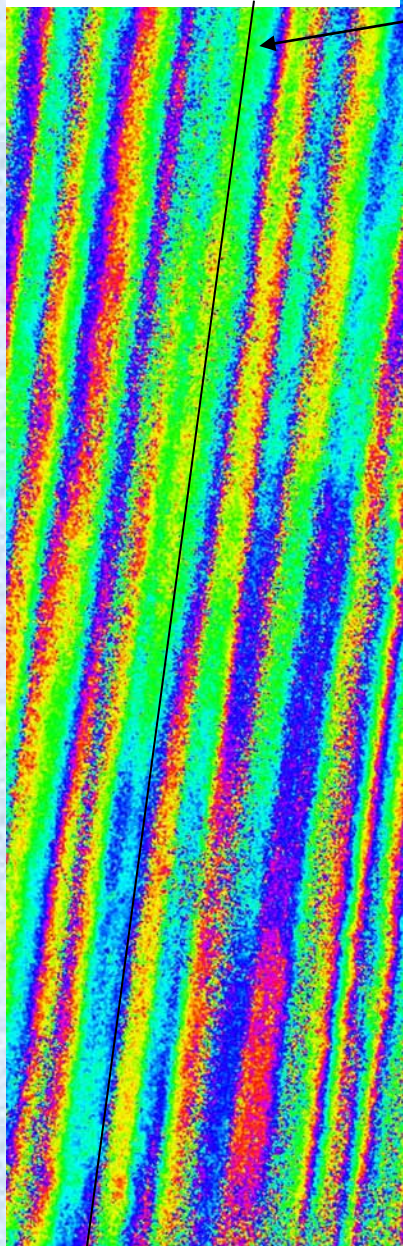


Total number of appearance : 1490 : June 2006~Dec. 2009

Amplitude image
(hh polarization)
2006/11/05



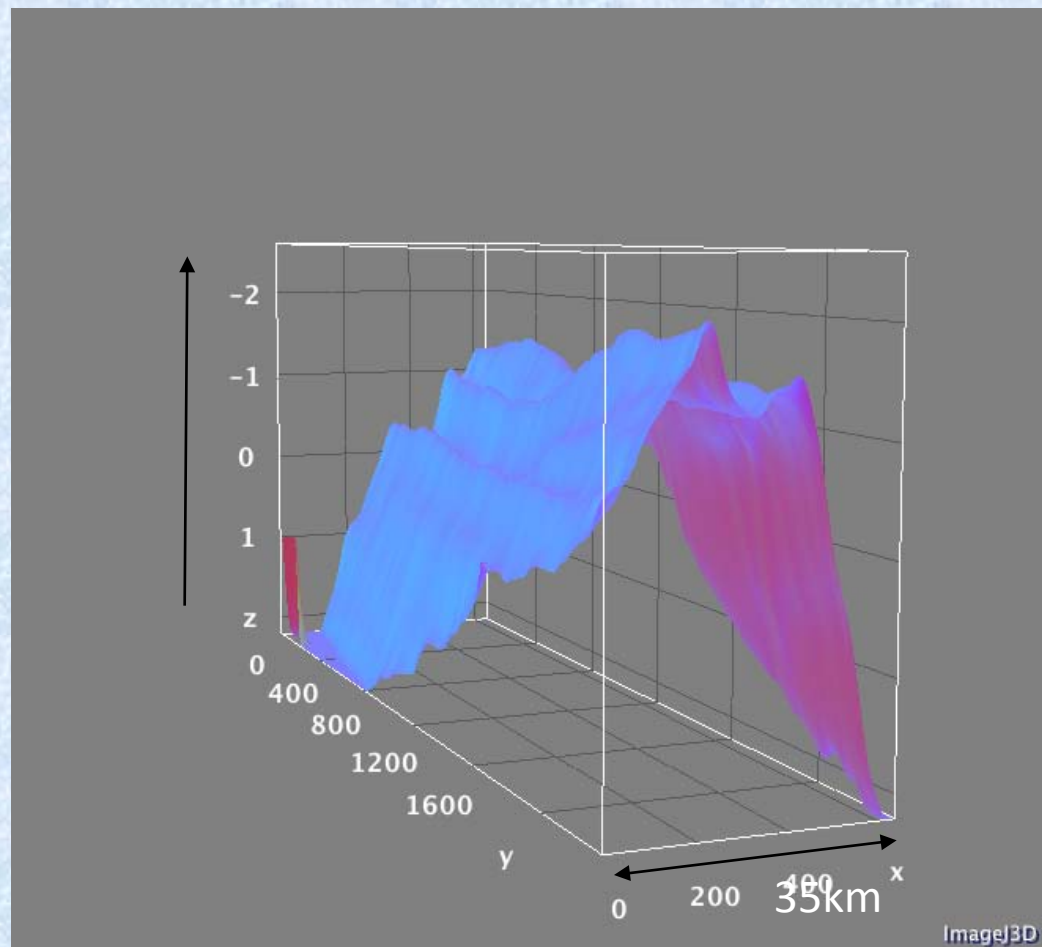
Phase (orbit and
terrain corrected
phase)



One example of lower latitude case in Brazil

Direction of the line – parallel to the
geomagnetic line

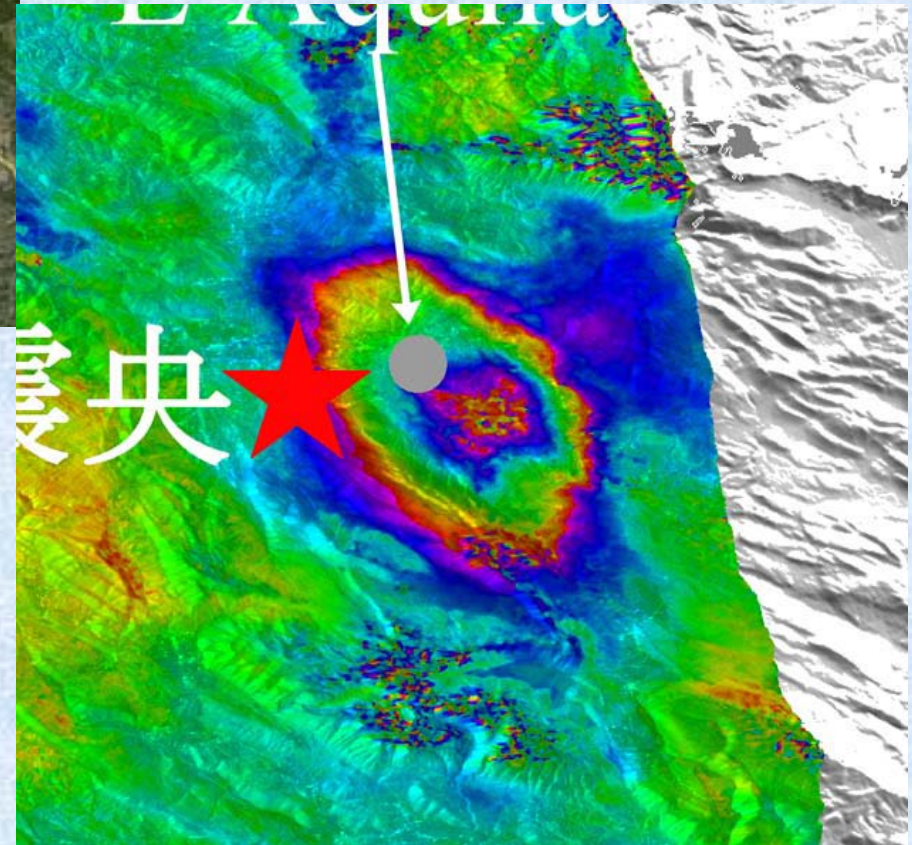
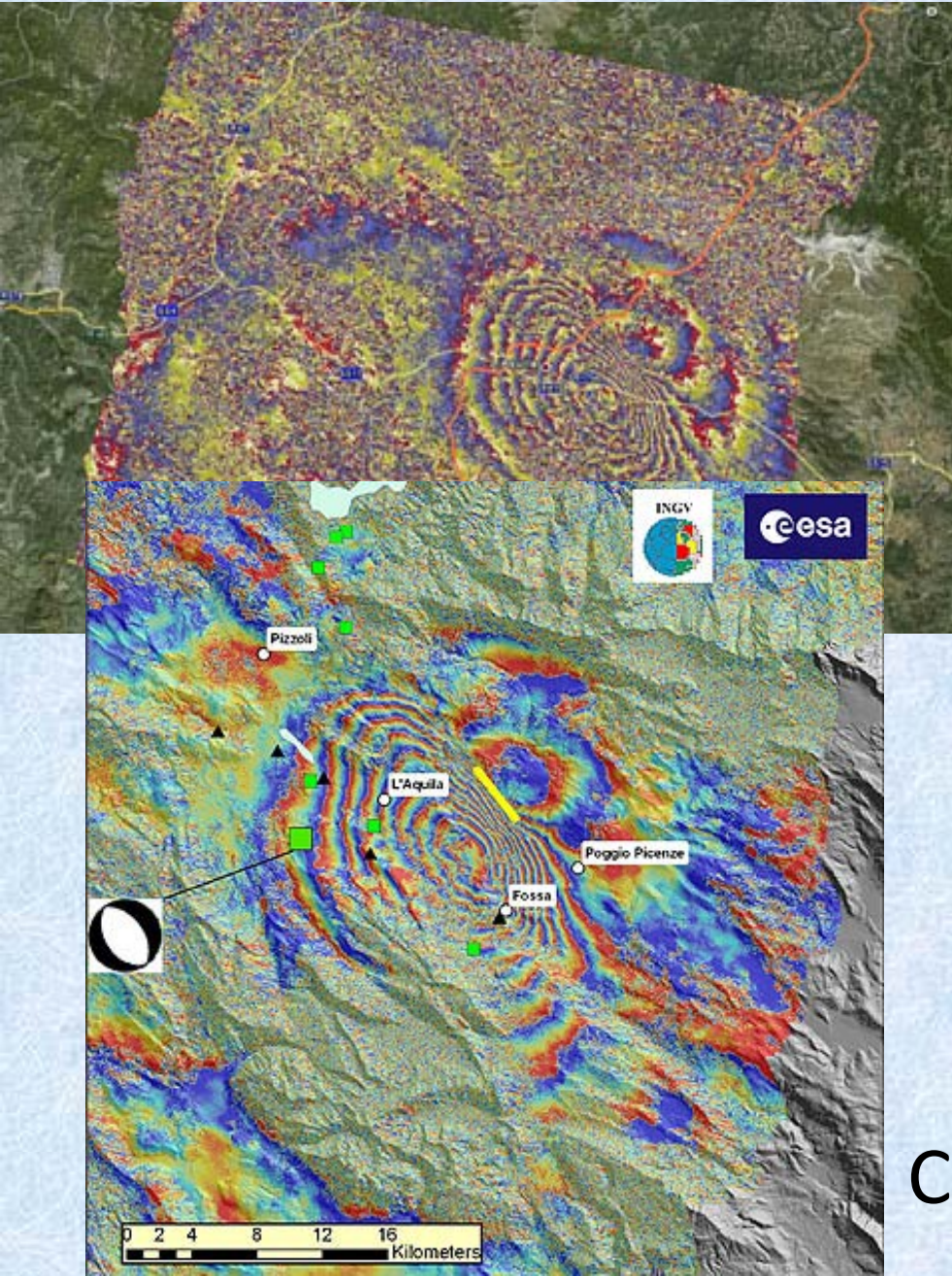
20060920-20061105:RSP072:Brazil



Unwrapped phase

Three Frequency SAR for L'Aquila Earthquake

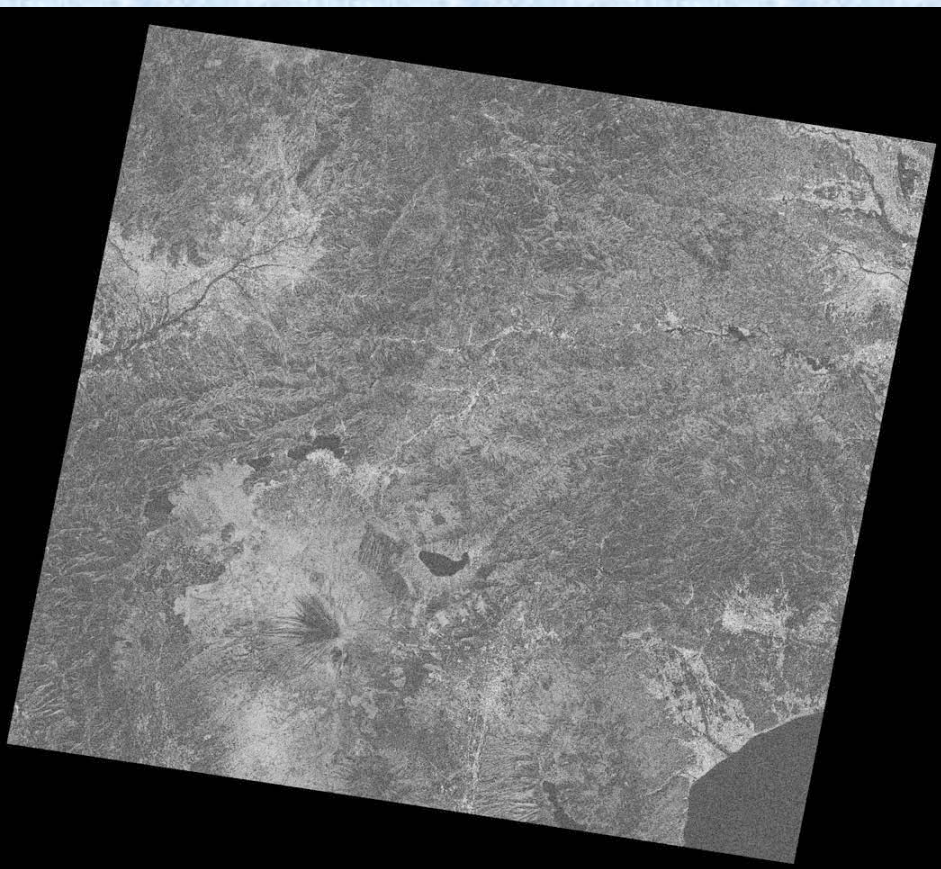
X イタリア地震



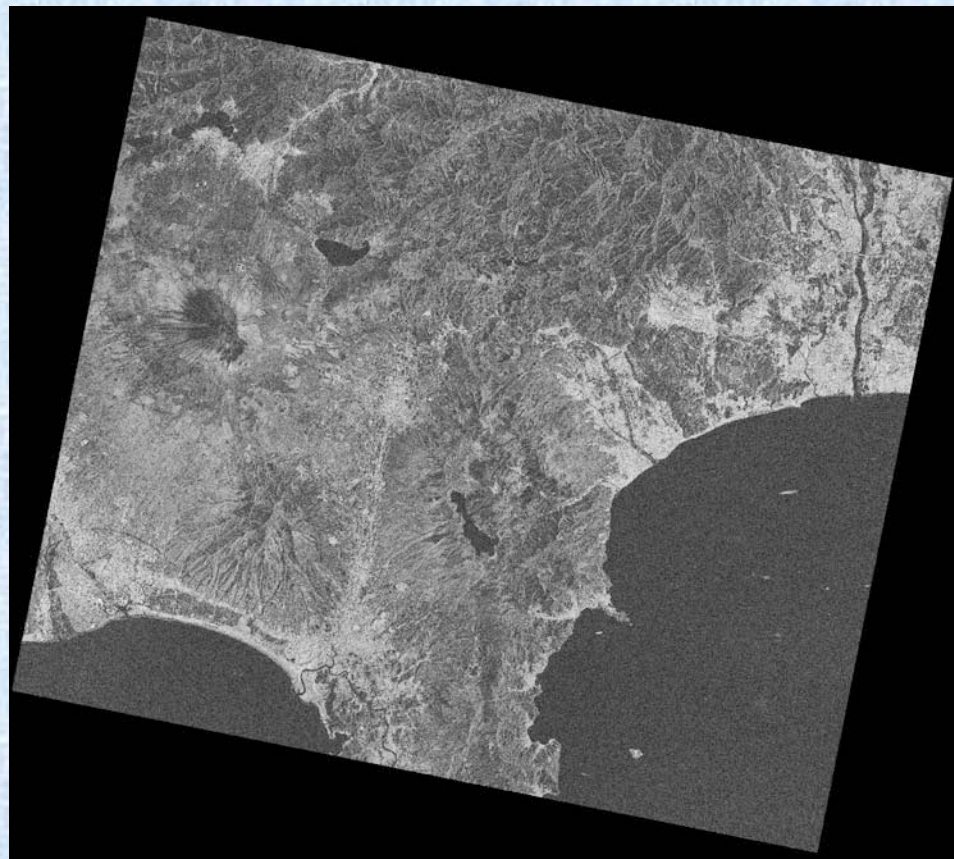
C

L

Comparison of JERS-1 SAR + PALSAR(34.3) in coherence



JERS-1 SAR
Oct. 21 and Sept. 7, 1995.

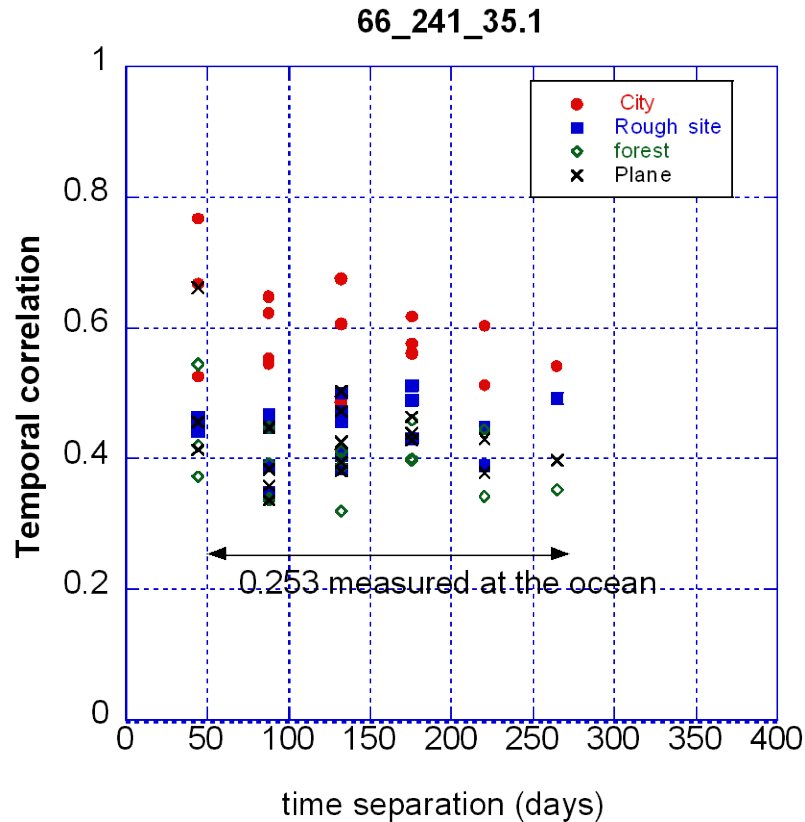
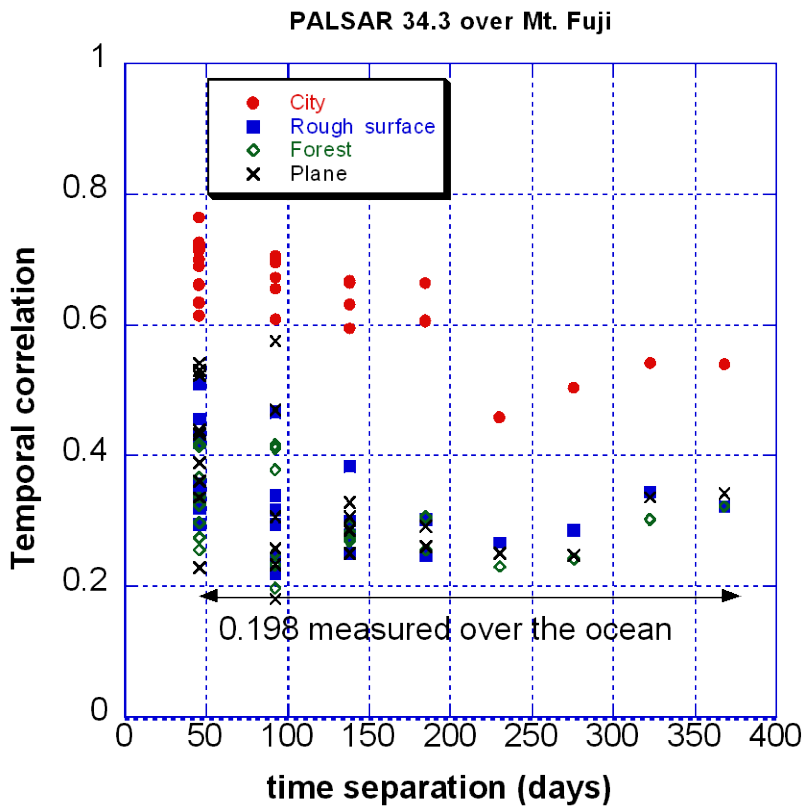


PALSAR

JERS-1 SAR/PALSAR Coherence Comparison

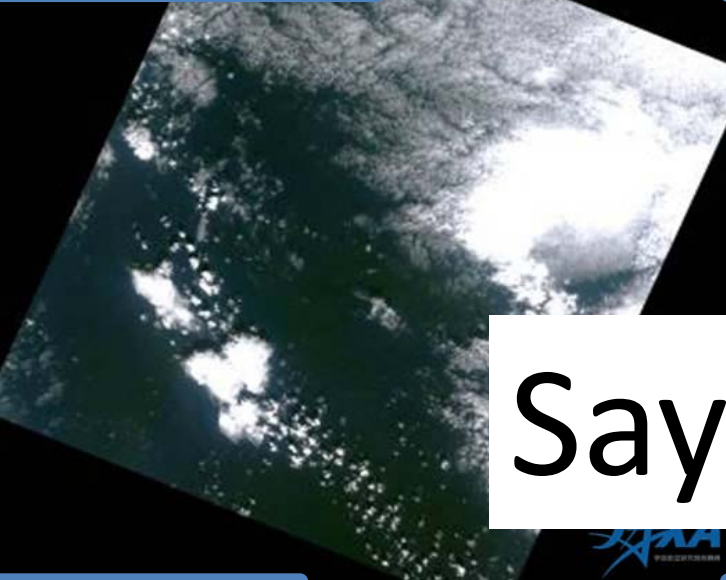
PALSAR

JERS-1 SAR



Noise level: higher in JERS-1
Dynamic range: smaller in JERS-1

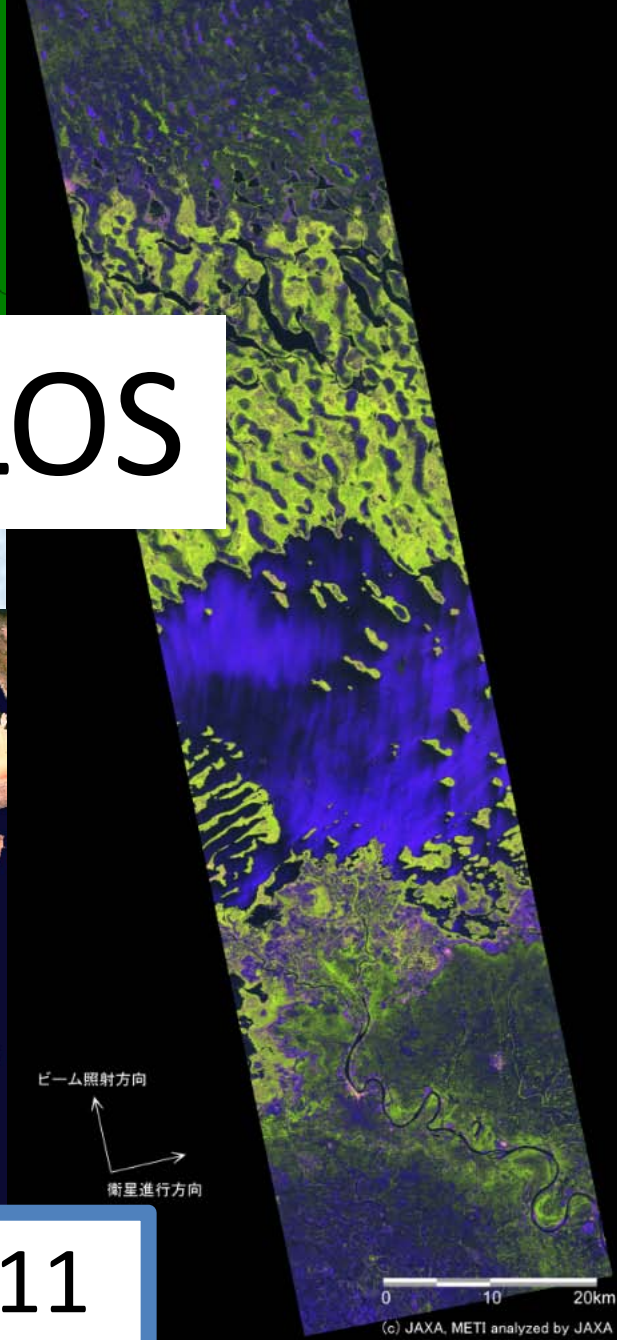
Final – AVNIR-2



AV2/PRISM-track

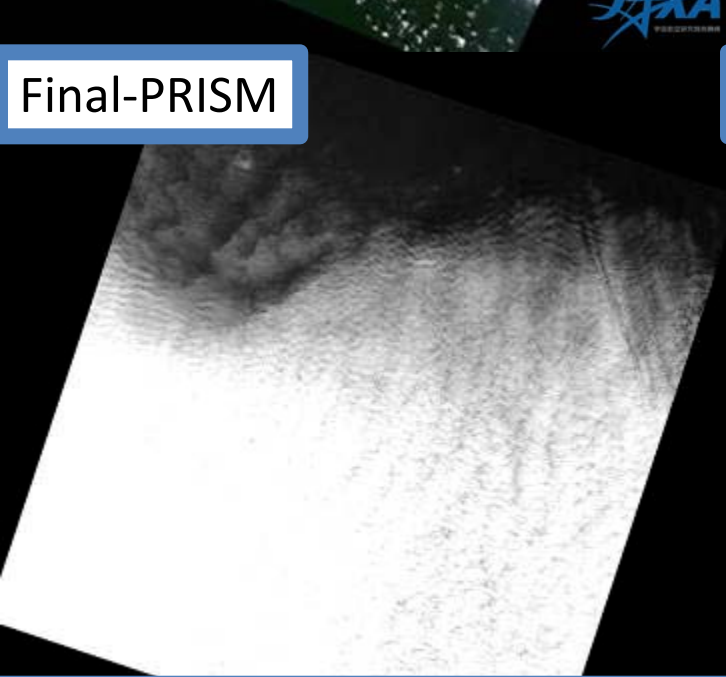


PALSAR - FULLPOL



Sayonara-ALOS

Final-PRISM



PALSAR-track



Final ALOS Images of April 22, 2011

0 10 20km

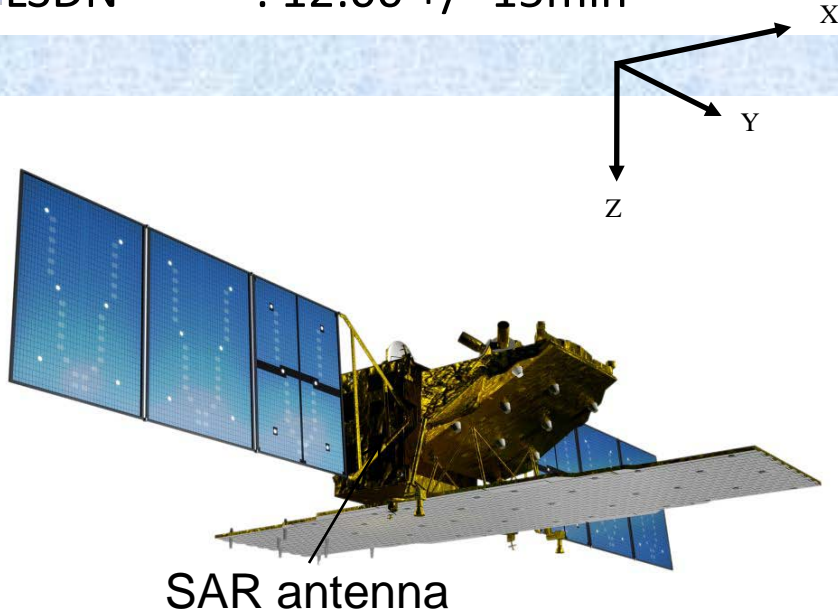
(c) JAXA, METI analyzed by JAXA



The ALOS-2

ALOS-2 satellite

- Orbit type : Sun-synchronous
- Launch : 2013
- Altitude : 628km +/- 500m(for reference orbit)
- Revisit time : 14days
- LSDN : 12:00 +/- 15min



PALSAR-2

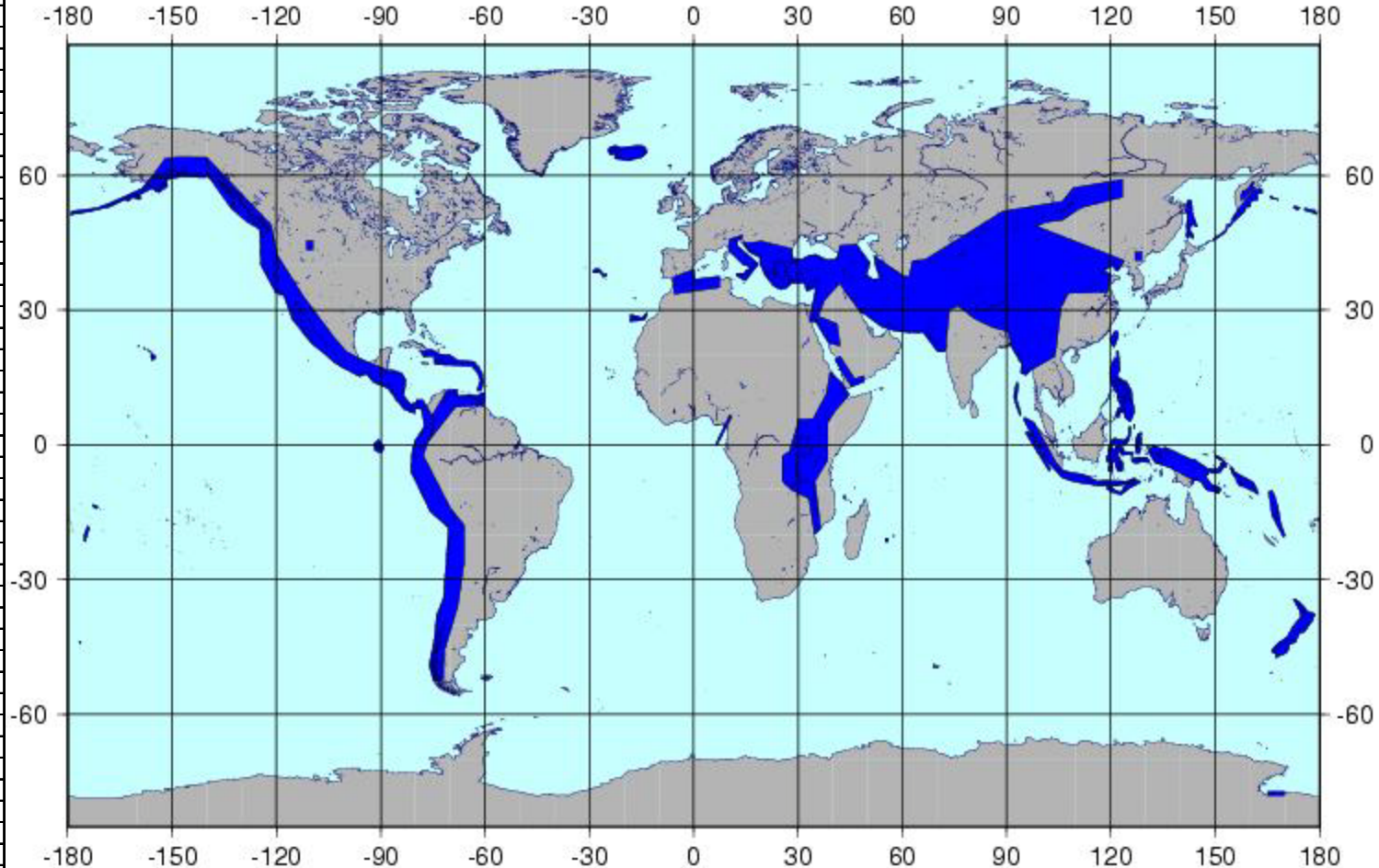
- L-band Synthetic Aperture Radar
- Active Phased Array Antenna type
two dimensions scan (range and azimuth)
- Antenna size : 3m(EI) x 10m(Az)
- Bandwidth : 14 to 84MHz
- Peak transmit Power : 5100W
- Observation swath : 25km to 490km
- Resolution : Range 3m to 100m
Azimuth 1m to 100m

RA: July 2012

Observation Region for deformation 1/2

FBD 【10m】, 28MHz

エリア
Eurasia
Algeria
Italy
Baekdu
Sakhalin
Kuril
KurilVolc
NewZealand
Iceland
Timor
Sumatra
SumatraWest
Andaman
Celebes
Talaud
Moluccas
Seram
NewGuinea
Vanuatu
Philippine
Taiwan
Alaska
NorthAmerica
SouthAmerica
Yellow
Venezuela
Cuba
SaudiVolc
YemenVolc
G RiftValley
CameroonVolc
Comoros
AleutianWest1
AleutianWest2
AleutianEast
Galapagos
Hawaii
Tonga
Samoa
SolomonIslands
KanaryIslands
Azores
Reunion
Erebus



● 高分解能[10m]モード

● 入射角: 30度~45度

● 降交軌道左右方向で年1回観測 (火山活動が活発な時期は年2回観測する。)

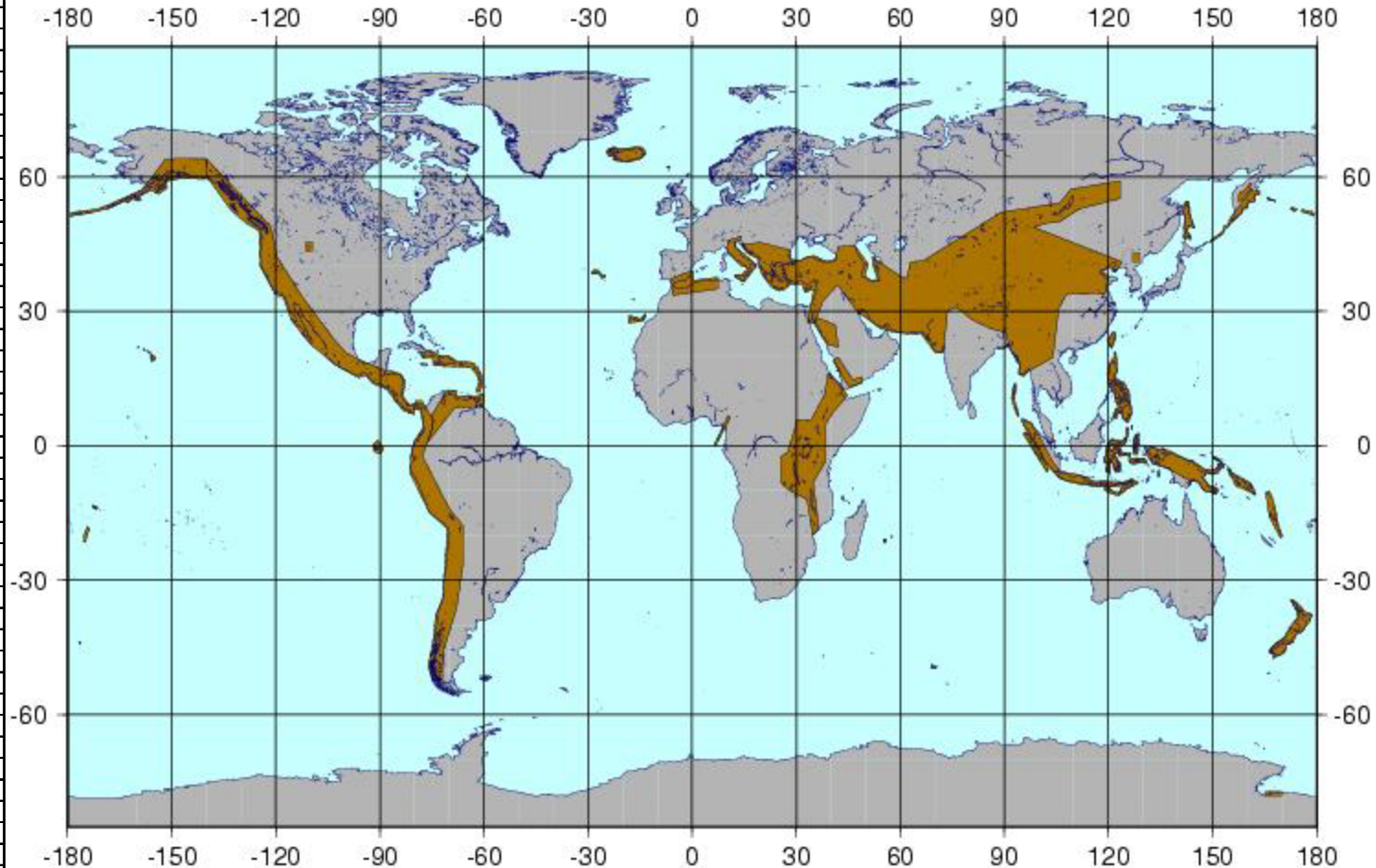
• Left/right tilting of satellite is a demanding manoeuvre, I would suggest instead acquisitions in ascending and descending passes.

• 10mモード HH+HV

Observation Region for deformation 1/2

ScanSAR 14 MHz Dual

Eurasia
Algeria
Italy
Baekdu
Sakhalin
Kuril
KurilVolc
NewZealand
Iceland
Timor
Sumatra
SumatraWest
Andaman
Celebes
Talaud
Moluccas
Seram
NewGuinea
Vanuatu
Philippine
Taiwan
Alaska
NorthAmerica
SouthAmerica
Yellow
Venezuela
Cuba
SaudiVolc
YemenVolc
G RiftValley
CameroonVolc
Comoros
AleutianWest1
AleutianWest2
AleutianEast
Galapagos
Hawaii
Tonga
Samoa
SolomonIslands
KanaryIslands
Azores
Reunion
Erebus



● 広域観測モード、14MHzで年1回

● 入射角:30度~45度

● 降交軌道左右方向で年1回観測 (火山活動が活発な時期は年2回観測する。)

基本観測計画

- 1) 変化抽出: 異なる入射角から要求後最短時間で観測:
ベースマップの作成とアップデート
- 2) 地殻変動: 同じ入射角から要求後最短時間で観測:
ベースマップの作成: 二つの要求が運用を困難に: $D+R+L$
に固執すると、観測頻度が極端に減少、広帯域の良好な
特性が時間劣化を補償出来ない。Scan-InSARとStrip-
InSARのバランス。
森林観測: 定期的な観測、ScanSAR+Dualと10mFBDがコア

現在、シミュレーションはスタート、2月末に一回目の結果を得る。同時並行に観測計画(戦略)をたてる。

Summary

ALOS observed the Earth repeatedly using L-band SAR, PALSAR, for five years and showed the L-band based repeat-pass interferometry performance on deformation, subsidence, volcanic monitoring.

ALOS-2, 2013, considers the InSAR in a way that

- 1. Orbit tube is +/- 500m (orbital maintenance every 3~4 months)**
- 2. Scan-InSAR will be globally used.**
- 3. (Right+Left looking in descending will be used for deformation monitoring.)**
- 4. Ascending for Forest monitoring**